Investigating the function of TRAF1 in NF-κB activation

Yitian Tang

A THESIS SUBMITTED TO

THE FACULTY OF GRADUATE STUDIES

IN PARTIAL FULFILLMENT OF THE REQUIREMENTS

FOR THE DEGREE OF

MASTER OF SCIENCE

GRADUATE PROGRAM IN KINESIOLOGY AND HEALTH SCIENCE

YORK UNIVERSITY

TORONTO, ONTARIO

December 2022

Abstract

Tumour necrosis factor receptor-associated factor (TRAF) proteins play an important role in mediating the activation of NF-κB. Dysregulation of NF-κB may be one of the potential causes of chronic inflammatory diseases. One member of the TRAF family, TRAF1, has been shown to increase the risk of rheumatoid arthritis (RA). However, TRAF1 plays opposing roles in the activation of NF-κB downstream of the tumour necrosis factor receptors (TNFR) and toll-like receptors (TLR) signalling pathways. In the TNFR pathway, TRAF1 recruits c-IAP2 to promote NF-κB activation and cell proliferation. In contrast, in TLR pathways, TRAF1 negatively regulates NF-κB by sequestering the linear ubiquitin assembly complex (LUBAC). Because of the complex role of TRAF1 in NF-κB activation, it is important to isolate and study the role of TRAF1 in each of these pathways. To better understand TRAF1 and its role in NF-κB activation, our laboratory has identified the same interaction site between TRAF1 and c-IAP2 and created a mutant TRAF1V203A that significantly reduces the interaction with c-IAP2. This study creates a working functional assay to test the effect of these mutants on NF-κB activation. We have generated TRAF1V203A knock-in monocyte THP-1 cells and demonstrated how this mutant alters signalling downstream of TLR and TNFR in monocytes. This study also shows that the production of pro-inflammatory cytokines is reduced in TRAF1V203A mutant monocytes. This study helps us to isolate effects on NF-κB activation and provides an excellent model to study the role of TRAF1 in vivo.

Acknowledgement

First and foremost, I would like to thank my supervisor Dr. Ali Abdul-Sater for giving me this opportunity to be a part of his wonderful lab and work on this project. Thanks to your guidance, support and advice carried me through this whole journey. Without your brilliant comments and suggestions everything would not have been possible.

Thanks should also go to Fatemah A, Mayoorey M, Safour Z, Sunpreet S, Jonathan R, Amandeep A, Ali A and Ali M for teaching and/or assisting me with the experiments. I would also like to thank my thesis committee members, Dr. Olasunkanmi Adegoke and Dr. Andrea Josse for their valuable time and contribution to complete my thesis.

I am also grateful to my parents for their support, appreciation and encouragement throughout my life.

And lastly, to my caring and supportive partner Francine and our beloved Luke, Leia and Lun: my deepest gratitude. Thank you for your love, company and helping me every step of this journey.

Table of Contents:

List of Figures

List of Tables

List of Abbreviations:

ACPA	Anti-citrullinated protein antibody
BIR	Baculoviral IAP repeat
cIAP	Cellular inhibitor of apoptosis protein
DAMP	Danger-associated molecular patterns
ERK	Extracellular signal-regulated kinase
FADD	Fas-associated death domain
HDR	Homology-Directed Repair
HOIL1	Heme-oxidized IRP2 ubiquitin ligase 1
HLA	Human leukocyte antigen
IAPs	Inhibitor of apoptosis proteins
IκB	Inhibitor of κB
IKK	IκB kinase complex
IL-1	Interleukin-1
IL-12	Interleukin-12
IL-1β	Interleukin-1β
IL-6	Interleukin-6
IRF	Interferon-regulatory factors
JNK	c-Jun N-terminal kinase
K48-Ub	K48-linked polyubiquitination
K63-Ub	K63-linked polyubiquitination
LPS	Lipopolysaccharide
LRRs	Leucine-rich repeats
LUBAC	Linear ubiquitin chain assemble complex
MAPK	Mitogen- activated protein kinase
M1 Ub	Linear polyubiquitination
MyD88	Myeloid differentiation primary response 88
NEMO	NF-κB essential modulator
NF-κB	Nuclear factor κB
NLRP3	NLR family pyrin domain containing 3
NLRs	NOD -like receptors
NOD	Nucleotide binding-oligomerization domain
PAMP	Pathogen-associated molecular patterns
PRRs	Pattern-recognition receptors
RA	Rheumatoid Arthritis
RF	Rheumatoid Arthritis Factor

RIG-I	Retinoic acid-inducible gene I
RIP1	Receptor-interacting protein I
RLRs	RIG-I-like receptors
SgRNA	Synthetic guide RNA
SNP	Single nucleotide polymorphism
TAB	TGF-beta-activated kinase 1 and MAP3K7-binding protein
TAK	Transforming growth factor-β activated kinase
TCR	T-cell receptor
TLR	Toll-like receptor
TNF	The tumor necrosis factor
TNFR	Tumor necrosis factor receptor
TRADD	Tumor necrosis factor receptor type 1-associated DEATH domain protein
TRAF	Tumor necrosis factor receptor -associated factor
Ub	Ubiquitination
WT	Wild type

Chapter 1: Literature Review

1.1 Autoimmune Disease and Rheumatoid Arthritis

The typical autoimmune disease condition results from an abnormal immune response wherein immune cells attack the body's own tissues and cells. The treatment for autoimmune disease, including nonsteroidal anti-inflammatory drugs (NSAIDs), immunosuppressants, and intravenous immunoglobulin, depend on the type and severity of the condition [34]. Rheumatoid arthritis (RA) is a chronic autoimmune disorder characterized by joint capsule inflammation. Other tissues may also be damaged in RA, including the skin, eyes, lungs, and heart [1]. Notably, although the various therapies mentioned above are highly efficient, many patients still do not respond to these therapies or become refractory to treatment. Hence, a better understanding of the mechanism that causes joint inflammation may be essential to identify new therapies for RA. Despite the cause of RA remaining unclear, the underlying mechanism indicates that the immune system is attacking the bone and cartilage by accumulating immune cells (i.e., monocytes, macrophages, and activated T and B cells) [1]. One of the currently used diagnostic biomarkers of RA is autoantibodies, which can be found in the serum and synovial fluid of RA patients [16]. Autoantibodies include rheumatoid factor, anti-citrullinated protein antibodies (ACPA), and anti-carbamylated protein antibodies (anti-CarP antibodies) [16]. These are specific to many autoantigens and can be induced by

various mechanisms, including promoting uncontrolled neutrophil activation and inducing inflammation [58]. Autoantibodies may form immune complexes in the joints and release chemotactic factors to establish a chemotactic gradient and recruit immune cells, which can cause chronic inflammation and bone destruction [15].

Furthermore, a genome-wide analysis of RA-associated genes found that the human leukocyte antigen (HLA)-DRB1 locus is responsible for autoreactive immune response by affecting T cell selection and antigen presentation [59]. Although HLA-DRB1 are well-established susceptibility loci, TRAF1-C5 has also recently been identified as a risk locus for RA. Another genome-wide association analysis identified that a genetic variant at the TRAF1-C5 locus on chromosome 9 is associated with an increased risk of RA [15]. In addition, a serum study found that the concentration of TRAF1 in RA patients is significantly higher than in healthy people [60]. Since TRAF1 is involved in the nuclear factor-κB (NF-κB)-dependent signalling pathway, understanding its involvement in both innate and adaptive immune response is important.

1.2 Nuclear Factor-κB and inflammatory response

NF-κB is a protein complex that regulates multiple aspects of cellular functions, such as cellular growth, inflammatory response, and apoptosis. As a master transcription factor, NF-κB not only induces the expression of multiple pro-inflammatory genes that encode

cytokines and chemokines but also plays a critical role in regulating cell proliferation, activation, and differentiation of innate immune cells and inflammatory T cells. In addition, NF-κB is involved in NLRP3 inflammasome regulation [2,3,4]. NLRP3 inflammasomes are multiprotein oligomers of the innate immune system that assemble in the intracellular cytosol after sensing pathogen-associated molecular patterns (PAMPs) or danger-associated molecular patterns (DAMPs) [66]. The activation of NLRP3 inflammasome requires two signals. First, NF-κB activation is promoted, and the expressions of NLRP3 protein and pro-IL-1β are elevated [12, 69]. To fully activate NLRP3, the activation of the NLRP3 signal can be provided by various stimuli, including extracellular ATP, reactive oxygen species (ROS), and calcium influx [68]. Upon detection of these two signals, NLRP3 forms the platform for recruiting and cleaving caspase-1. Caspase-1 within the activated NLRP3 can further activate the pro-inflammatory cytokine IL-1β [69]. Therefore, aberrated NF-κB activation contributes to the pathogenic process of several inflammatory disorders, such as RA.

The NF-κB family is composed of five different members, namely, NF-κB1 (or p50), NF-κB2 (or p52), RelA (or p65), RelB, and c-Rel. NF-κB can act as a transcription factor when its subunits form homo- or heterodimers [3,4]. In addition, NF-κB can be activated by various stimulants, including inflammatory cytokines, bacterial toxins (such as lipopolysaccharides), and mitogens [47].

When NF-κB is in an inactivated state, it is located in the cytosol and is inhibited by the inhibitory protein IκBα [8]. NF-κB can be activated by canonical and non-canonical pathways. A typical structure of the NF-κB complex in the canonical pathway is the p50/p65 complex [19]. Meanwhile, the non-canonical pathway is predominantly caused by the activation of the p52/RelB complex [48].

The canonical NF-κB pathway responds to various stimuli, including pattern-recognition receptors (PRRs), TNF receptor (TNFR) superfamily members, and T-cell and B-cell receptors [8]. In this pathway, NF-κB is activated by IκBα degradation through phosphorylation by I**κB** kinase (IKK), resulting in nuclear translocation and activation of the target genes [6]. IKK is an enzyme complex composed of three subunits, namely, IKKα, IKKβ, and the regulatory submit IKKγ (known as NEMO). Specifically, IKK phosphorylates IκBα, which leads to K48-linked polyubiquitination, resulting in the dissociation of IκBα from NF-κB. After IκBα releases NF-κB, it translocates into the nucleus and changes the cellular function [20].

Unlike the canonical pathway, the non-canonical pathway responds to the subset of TNFR signals, including CD40, the B-cell-activating factor belonging to the TNF family receptor (BAFFR), the lymphotoxin β-receptor (LTβR), and the receptor activator for the nuclear factor κB (RANK). The activation of the non-canonical pathway relies on the phosphorylation of p100 instead of the degradation of IκBα [48]. TRAF3 continuously ubiquitinates the NF-κB-inducing kinase (NIK) at a steady state. However, the

degradation of TRAF3 prevents the ubiquitination of NIK and allows the accumulation of newly synthesized NIK. NIK further phosphorylates p100 and forms p52/RelB heterodimers [48, 49].

1.3 Ubiquitination and protein regulation

Protein ubiquitination is a post-translational modification that degrades proteins and recycles the substrates. This modification has various functions, including cell signalling, apoptosis, protein processing, immune response, and DNA repair [50].

Ubiquitin is a small regulatory protein consisting of only 76 amino acids [37]. The addition of ubiquitin to a substrate protein is called ubiquitination. This reaction requires three different enzymes: ubiquitin-activating enzyme (E1), ubiquitin-conjugating enzyme (E2), and ubiquitin-protein ligase (E3) [38,39].

Ubiquitination involves three steps. First, E1 loads ubiquitin between the C-terminal carboxyl group of ubiquitin and the cysteine group of the ubiquitin-activating enzyme in an ATP-dependent manner. Second, E2 transfers ubiquitin from the E1 site to its active site and then carries ubiquitin to the cellular proteins. Third, E3 interacts with E2 and mediates the transfer of ubiquitin from E2 to the target protein [43,50,51,53]. Ubiquitin modification can be reversed by deubiquitinating enzymes (DUBs) by cleaving ubiquitin from the target protein [54].

The most common ubiquitin modification is K48-linked ubiquitination, which targets proteins to the proteasome for degradation. The second most common form is K63-linked ubiquitination, whose role is to provide platforms for cell signalling. Moreover, Met-1-linked ubiquitin chains are generated when ubiquitin molecules attach to the N-terminal amino group of methionine. They are catalyzed by the linear ubiquitin chain assembly complex (LUBAC) and play an essential role in regulating the inflammatory cell signalling pathway in both innate and adaptive responses [43].

1.4 Tumour Necrosis Factor Receptors (TNFRs) Superfamily and TNFR-associated factors (TRAFs)

The TNFR superfamily is a group of cytokine receptors that can bind to TNFs via an extracellular cysteine-rich domain [40]. TNF receptors are expressed in a wide range of mammal tissue and are involved in apoptosis, inflammation, proliferation, survival, and differentiation [45]. The TNFR superfamily can be categorized into two groups according to the presence or absence of a death domain. Since these receptors do not have kinase activity, most TNFRs require specific adaptor proteins, such as TRAFs, TRADD (Tumor necrosis factor receptor type 1-associated DEATH domain protein), RIP (receptor-interacting protein), and FADD, for downstream signalling. In TNFR1, binding with its adaptor protein TRADD allows the activation of the NF-κB or cell death pathway [41].

TNFR1 activation leads to the formation of two different signalling complexes. Complex I controls the expression of survival signal and prevents cell death via NF-κB activation, thereby inhibiting complex II formation. However, TNFR1 switches from pro-survival to pro-death when NF-κB activation is impaired by forming complex II by activating caspase-8 [41].

TRAFs are a family of proteins involved in various immune responses, such as inflammation, antiviral responses, and apoptosis. As adaptor proteins, they can mediate the interaction between upstream receptors and downstream effector molecules by forming a receptor-associated signalling complex [35]. Researchers have found that some TRAF members act as E3 ubiquitin ligases and can activate transcription factors, such as NF-κB, mitogen-activated protein kinases (MAPKs, ERK-1 and ERK-2, JNK, and p38), and interferon-regulatory factors (IRF3 and IRF7) [3]. The mammalian TRAF family has six members; only TRAF1 lacks a RING-finger domain [22]. Although TRAF1 is missing a RING finger domain, it still plays a critical role in the NF-κB and MAPK signalling pathways. Several studies have proven that the role of TRAF1 in NF-κB activation is peculiar, indicating that TRAF1 has both positive and negative effects on NF-κB activation [23,45]. These contrary results have shown that TRAF1-regulated NF-κB is highly dependent on the cell type and receptor being stimulated. Since RA is a complex autoimmune disorder that involves multiple immune cell types, such as macrophages, lymphocytes, and monocytes, understanding the role of TRAF1 is extremely important.

1.5 TRAF1 signaling downstream of Tumor Necrosis Factor Receptor 1 (TNFR1)

Once TNF binds to TNFR1 and interacts with the adaptor protein TRADD, it recruits TRAF2, c-IAP1/2, and RIP1 to form a complex, leading to the activation of NF-κB. This research found that TRAF1 is also involved in the recruitment of c-IAP by forming a heterotrimer with TRAF2. The formation of the TRAF1:(TRAF2)2 heterotrimer also increases the affinity to c-IAP2 compared with the TRAF2 homotrimer [42] (See Figure 1).

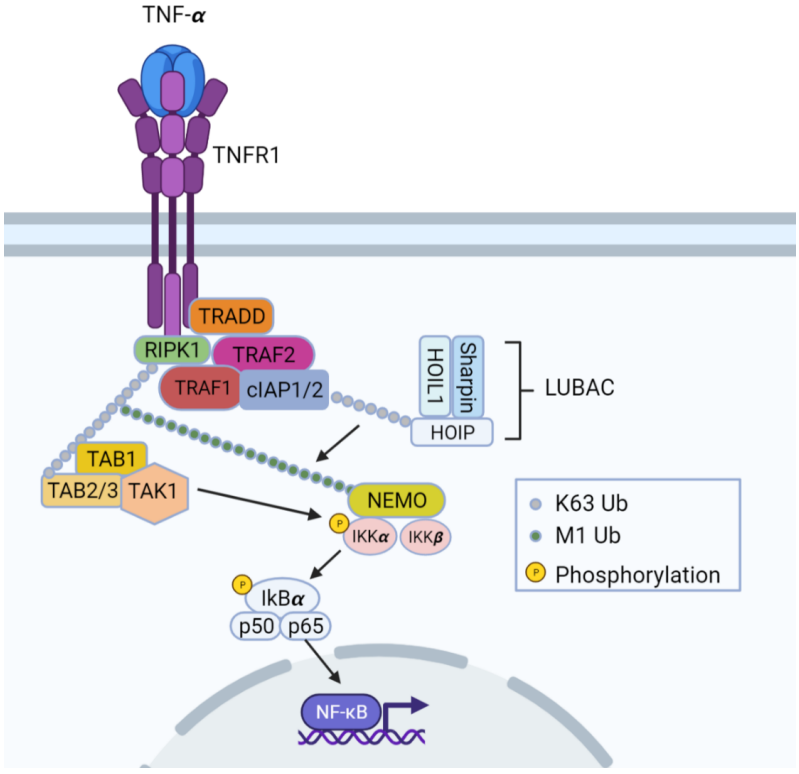

Figure 1. An overview of NF-κB activation downstream of TNFR1. TNFR1 recruits tumor necrosis factor receptor type 1-associated DEATH domain protein (TRADD), TRAF1 and TRAF2. TRAF complex further recruits cellular inhibitors of apoptosis protein (cIAP1 or 2). Ciap1/2 add K63-Ub to receptor-interacting protein I (RIP1) and recruits transforming growth factor-β activated kinase (TAK1) complex. The linear ubiquitin assembly complex (LUBAC) also recruits by K63-Ub and adds M1-Ub to recruit the IκB kinase (IKK) complex. Phosphorylation of IKK complex further phosphorylates inhibitor of Kb (IκB), which release nuclear factor κB (NF-κB) to nucleus. Image adapted from [33]

Accumulating data have shown that TRAF1 may have negative and positive TNF receptor functions, depending on the cell types. One study found that overexpression of TRAF1 in HEK293T cells can prevent NF-κB activation induced by TNF [26]. However, another study demonstrated that the overexpression of TRAF1 inhibits the antigen-induced apoptosis of CD8+ cells by promoting NF-κB activation [25]. This evidence suggests that TRAF1 plays a positive role in NF-κB activation in lymphocytes under normal physiological conditions. Therefore, the role of TRAF1 in signalling is highly dependent on cell types. It can promote NF-κB activation in TNFR downstream signalling in lymphocytes but also reduce NF-κB activation in TLR downstream signalling in monocytes.

1.6 Cellular inhibitor of apoptosis protein (c-IAP1/2)

The cellular inhibitor of apoptosis proteins 1 and 2 (cIAP1 and cIAP2) and the X chromosome-linked inhibitor of apoptosis protein (XIPA) are members of a family of inhibitors of apoptosis proteins (IAPs) that mitigate both intrinsic and extrinsic death signalling [36]. They inhibit caspase activity competitively through baculoviral IPA repeat (BIR) domains [36]. C-IAP2 can function as an E3 ubiquitin ligase and mediate K48- and K63-linked ubiquitination based on the substrate and the receptor [20]. Recently, studies found that ubiquitin ligase activity within c-IPA1/2 is critical in regulating NF-κB

signalling and programmed cell death in the TNF-α mediated signalling pathway [36]. As an E3 ubiquitin ligase, c-IAP1/2 can be recruited by adaptor protein TRADD and mediate the polyubiquitylation of its substrate protein RIP1. This polyubiquitination also prevents the formation of complex II in TNF-α-stimulated cells. Thus, cells missing both cIAP1 and 2 are sensitized to TNFα-mediated cell death [55]. However, non-canonical NF-κB activation is enhanced in unstimulated cells when either c-IAP1 or 2 is missing. Normally, non-canonical NF-κB activation is inhibited by TRAF2, TRAF3, and cIAP1/2 to maintain NIK at a low basal level. The interaction between NIK and TRAF2: cIAP1/2 complex can be lost when TRAF3 is degraded, resulting in the stabilization of newly synthesized NIK and NF-κB activation [36, 56].

1.7 TRAF1 signaling downstream of 4-1BB receptor in T cells

Within T cells, TRAF1 plays the role of a critical adaptor protein in the TNFR and 4-1BB downstream pathways [11]. The 4-1BB is part of the TNFR superfamily and is expressed in T cells. Several studies have confirmed that TRAF1 also acts as a positive regulator in 4-1BB signalling [27, 28]. The activation of the 4-1BB pathway leads to T cell proliferation and cytokine production [28] (See Figure 2).

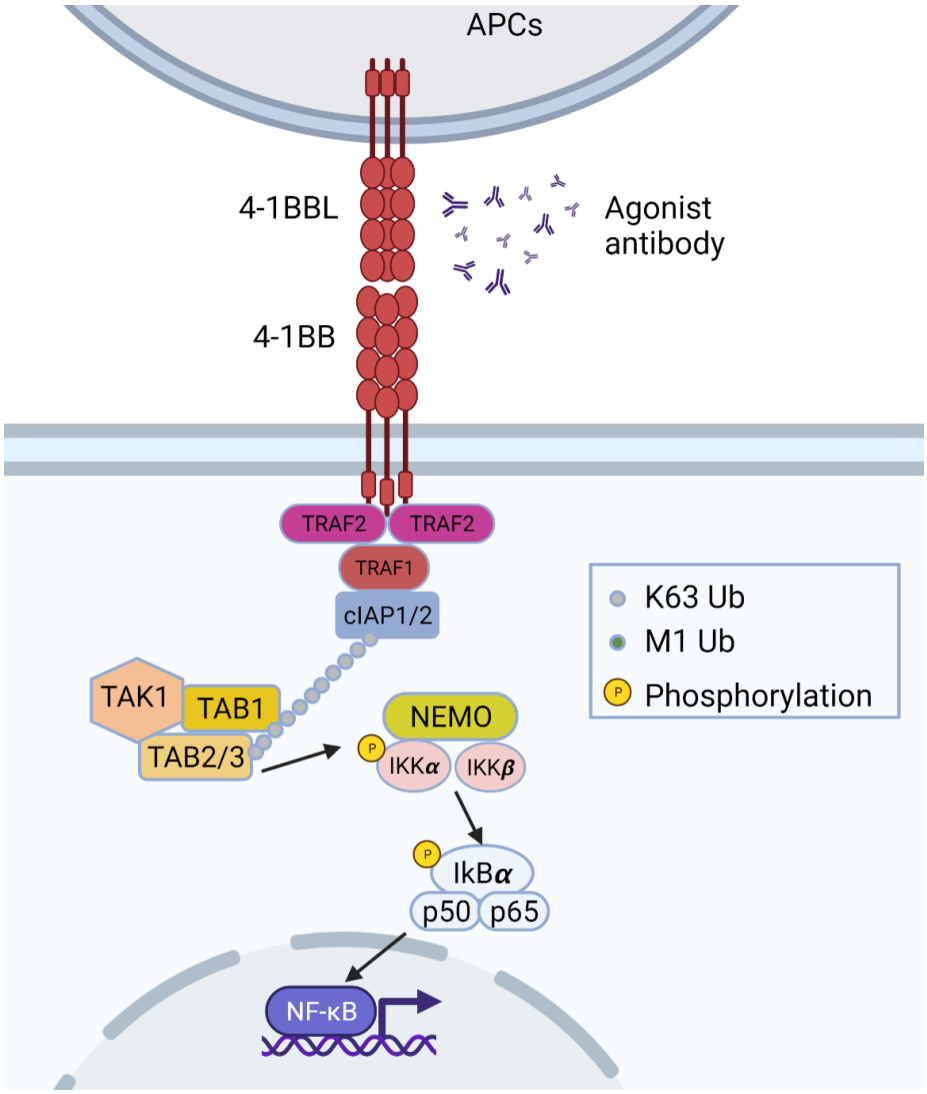

Figure 2. An overview of NF-κB activation downstream of 4-1BB. 4-1BB recruits TRAF1 and TRAF2 to form.a heterotrimer. The heterotrimer further recruits Ciap1/2 which further mediates the activation of downstream effectors. Image adapted from [29]

When 4-1BB binds to its ligand (4-1BBL), it recruits TRAF2 and TRAF1 to form a heterotrimer (TRAF1:$(TRAF2)_2$) [14]. The heterotrimer further recruits c-IAP1/2 and ubiquitinated TAK1, which leads to the phosphorylation of the IKK complex and NF-κB activation [29].

1.8 TRAF1 signalling downstream of TLR receptor

PRRs are mainly expressed by innate immune cells, such as dendritic cells, macrophages, monocytes, and neutrophils [30]. PRRs can recognize PAMPs and DAMPs. These receptors can promote the expression of chemokines, cytokines, antibacterial peptides, and interferons once activated. PRRs can be further categorized into several subgroups, including Toll-like receptors (TLRs), RIG-like receptors (RLRs), Nod-like receptors (NLRs), and C-type receptors (CLRs) [31]. TLRs consist of ectodomain leucine-rich repeats (LRRs) that are required for PAMP or DAMP recognition, a transmembrane domain, and a cytoplasmic Toll/Interleukin (IL)-1 receptor (TIR) domain that transmits the downstream signal [46].

As mentioned above, the canonical NF-κB pathway also responds to PRRs. Although TLRs are also involved in NF-κB signalling, they activate differently from the TNFRs downstream. Upon induction of TLRs, MyD88 is recruited to the TIR domain of the receptors and further recruited to the interleukin receptor-associated kinase 1/4 (IRAK1/4). After IRAK1/4 are autophosphorylated, they dissociate from MyD88 and interact with TRAF6. TRAF6 promotes Lys63-linked polyubiquitination of itself and other substrates, resulting in NF-κB activation [31,32] (see Figure 3).

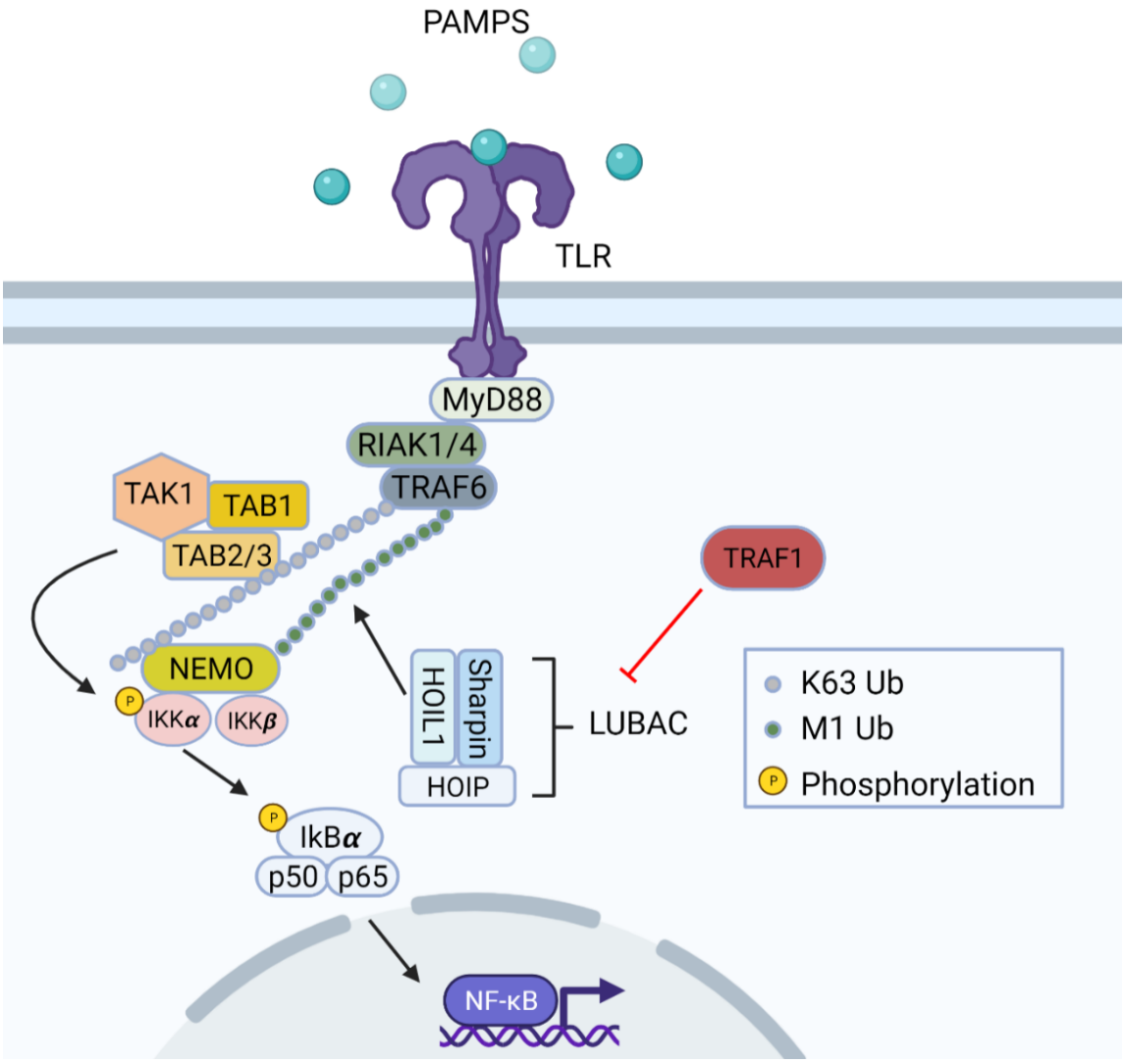

Figure 3. An overview of NF-κB activation downstream of TLR. TRAF1 inhibits the function of LUBAC and limiting NF-κB activation. Image adapted from [33]

The role of TRAF1 in the TLR pathway has been reported recently. A study based on the knockdown of TRAF1 in THP-1 cells showed increased NF-κB activation, which suggests that TRAF1 acts as a negative regulator [33]. TRAF1 interacts with the linear ubiquitin chain assembly complex (LUBAC) through its MATH domain [12]. The LUBAC complex activates NF-κB by forming M1-Ub chains and recruiting the IKK complex. However, the

linear ubiquitination of NEMO is reduced when TRAF1 interacts with LUBAC, which ultimately decreases the activation of NF-κB [13].

Chapter 2: Rationale and Objectives

2.1 Rationale

Dysregulation of NF-κB could be one of the potential causes of chronic inflammatory diseases such as RA. Multiple genetic studies have also found SNPs at the TRAF1-C5 locus are associated with an increased risk of RA. Both monocytes and T cells from healthy subjects with RA-associated SNP expressed less TRAF1 than normal SNP. Hence, TRAF1, a regulator of NF-κB pathway, could provide a potential therapeutic intervention for RA patients.

TRAF1 plays opposing roles in NF-κB activation downstream of the TNFR and TLR signalling pathways. At the same time, the pathogenesis of RA involves many immune cell types, such as lymphocytes and macrophages. In the TNFR pathway, TRAF1 recruits c-IAP2 to promote NF-κB activation and play an important role in T cell activation, proliferation and survival. On the contrary, in TLR pathways, TRAF1 is associated with LUBAC and decreases NF-κB activation and inflammatory cytokine production in macrophages. However, simply inhibiting TRAF1 as a therapy for RA is impossible because the exact mechanisms of TRAF1 is depends on types of immune cells. TRAF1 might downregulate NF-κB activation in TNFRs downstream but enhance NF-κB activation to TLR signalling. In this case, understanding the different mechanisms of

TRAF1 in TLR and TNFRs signalling seems to be the first step to developing a TRAF1-target therapy.

Our lab has identified the exact interaction site between TRAF1 with c-IAP2 and created a mutant TRAF1 V203A that significantly reduces the interaction with c-IAP2. However, whether this alters TRAF1 signalling has not been explored. This study aims to create a working functional assay to test the effect of these mutants on NF-κB activation. I will examine the function of mutated TRAF1 in monocytes and T cells. We have generated TRAF1V203A knock-in monocyte THP-1 cells by CRISPR/Cas9, and I will investigate how this mutant alters the signalling downstream of TLR, TNFR signalling and regulating inflammasome activation. Also, I will create TRAF1V203A knock-in Jurkat cells (T cells) by electroporation and study downstream of TNFR1 signalling.

2.2 Objectives:

The main objectives of the study are:

i. Assess the interaction between genetically modified TRAF1V203A and cIAP2 in the human monocytic cell line, THP1.
ii. Evaluate the effect of TRAF1V203A mutation to determine whether this abrogates the positive role of TRAF1 in inducing NF-κB signalling without altering its role in limiting linear ubiquitination.

iii. To create knock-in Jurkat T cells using CRISPR/Cas9 to modify the endogenous TRAF1 gene into TRAF1 V203A mutation.

2.3 Hypothesis:

I hypothesize that V203A mutation in TRAF1 that abrogates the interaction with c-IAP2 will downregulate the NF-κB activation in TNFR signalling while maintaining the same level of NF-κB in TLR signalling in monocytes. We also hypothesized that in V203A mutation in T cells will lead to a reduction of NF-κB activation in TNFR signalling.

Chapter 3: Experimental procedures

3.1 Cell culture

a) THP-1 cell line:

THP-1 cells are a human monocytic cell line. Wild type THP-1 and TRAF1V203A THP-1 were cultured in T75 flask at 37°C, 20% O2, and 5% CO2. Cells were kept in RPMI-1640 with 10% fetal bovine serum, 1% non-essential amino acids, 1% L-Glutamine-penicillin-Pyruvate-Streptomycin, and 0.1% 2-Mercaptoethanol. Media was replenished every 48 hours, and cells were split when grown to confluence. Cells were moved from T75 flask and placed into 50ml conical tubes and centrifuge at 1500RPM for 5 minutes at 4°C. After centrifugation, the media was removed, and cells were resuspended in fresh media.

a) Jurkat cell line:

Jurkat cells are human T lymphocyte cells. These cells follow the same steps as mentioned above for incubation and maintenance.

3.2 Collection of cell lysates

a) Cell lysates for TNF-αlpha induction experiment

THP-1 cells were collected and moved into 1.5ml ER tubes and centrifuged at 1500RPM for 5 minutes at 4°C. After the centrifugation, removed media and

washed the cell pellet with cold PBS and centrifuged again centrifuge at 1500RPM for 5 minutes at 4°C. After removing the PBS, cells were lysed with 100ul of freshly prepared 1x lysis buffer with 1% NP- 40, 100mM Tris pH 8.0, 20% glycerol, 0.2mM EDTA, 150mM NaCl, Complete 1x Protease Inhibitor Cocktail, 1x Phosphatase Inhibitor Cocktail, 1 mM DTT, ddH2O. Cells with lysis buffer were incubated on ice for 20 minutes with vortexing every 5 minutes. After the incubation, samples were centrifuged at 14000RPM for 15 minutes at 4°C. The supernatant was collected and stored at -80°C.

b) Cell lysates for co-immunoprecipitation

THP-1 cells were collected and moved into 15ml conical tubes and centrifuged at 1500RPM for 5 minutes at 4°C. After the centrifugation, removed media and washed the cell pellet with cold PBS and centrifuge again centrifuge at 1500RPM for 5 minutes at 4°C. Cells were lysed with 1ml of lysis buffer containing 20 mM Tris HCl pH 8, 137 mM NaCl, 10% glycerol, 1% NP-40, 2mM EDTA, Complete Protease Inhibitor Cocktail, PhosSTOP Phosphatase Inhibitor Cocktail, and 1 M DTT, and ddH2O. Lysates were obtained following the same procedure mentioned above.

c) Cell lysates for K63 Ubiquitin assay

THP-1 cells were collected and washed as mentioned above. Cells were lysed with 1ml of RIPA lysis buffer containing 50mM Tris-HCl pH8, 150mM NaCl,

1% NP-40, 0.1% SDS(Sodium Dodecyl Sulfate), 0.5% DOC(sodium deoxycholate), and ddH2O. Lysates were obtained following the same procedure mentioned above.

3.3 Bradford Protein Assay

Bradford standard was determined with 1mg/ml of BSA via serial dilution. 872ul of Bradford reagent (sigma) was mixed with 128ul of the BSA, then 500ul of this mixture was transferred to the second ER tube and mixed with 500ul of Bradford reagent. This procedure was repeated five times until concentrations of 64μg/ml, 32μg/ml, 16μg/ml, 8μg/ml, and 4μg/ml were achieved. 5ul of samples is mixed with 500ul of Bradford reagent and transferred to a 96-well plate in duplicates. Absorption was measured at 595nm wavelength and calculated the concentration of the samples.

3.4 Co-immunoprecipitation

The cell lysate was obtained as mentioned above. 15ul of lysate was saved and used for input. 1.5ug of anti-TRAF1 antibody (clone 1F3) was added and incubated with protineA/G agarose beads (Thermo Scientific) at RT for 10 min on a rotator. 950ul of lysate was incubated with 20ul of antibody-bonded beads for 2h at RT on a rotator. After the

incubation, beads were washed three times with 1x CO-IP lysis buffer and PBS twice. Lastly, the beads were eluted with 20ul of 2X Laemmeli Buffer.

3.5 K63 Ubiquitin Assay

Cell lysate was obtained as mentioned above. 15ul of lysate was saved and used for input. 2.5ug of cleaved caspase-1 antibody (D57A2) was incubated with proteinA/G agarose beads as mentioned above. Each lysate was incubated with 25ul of antibody-bonded beads overnight at RT on a rotator. After the incubation, beads were washed with 1ml of RIAP lysis buffer five times and two times with PBS. Lastly, the beads were eluted with 30ul of 2X NuPAGE LDS Sample buffer Invitrogen). 2X LDS sample loading buffer was diluted from 4x stock with ddH2O and containing 5mM DTT. Samples were heated at 70°C for 10min, then loaded onto 4-15% gradient SDS-PAGE gels and ran at 60V for 30 minutes and 12V for 90 minutes. After the electrophoresis, SDS-PAGE gels were transferred to nitrocellulose membranes (BioRad) through wet transfer method at 30V for two hours and blocked with 5% skim milk/TBST for one hour with shaking. The membrane was further incubated with anti K63 antibody(Millipore) with 1:1000 dilution for one hour at RT and incubated with secondary antibody with 1:10000 dilution for one hour. Blots were imaged using SuperSignal West Femto Substrate (Thermo Scientific).

3.6 Immunoblotting

Samples were prepared based on measured concentration and heated at 100°C for 5 minutes. Then, samples were loaded onto 10% SDS-PAGE gels and ran at 60 V for 30 minutes and 120 V for 90 minutes. After the electrophoresis, SDS-PAGE gels were transferred to PVDF membranes (BioRad) and blocked with 5% skim milk for one hour. The membrane was further incubated with a primary antibody with 1:1000 dilution at 4°C overnight and incubated with a secondary antibody (1:10000 dilution) on the following day. The substrate for immunoblotting were shown in this table:

Primary Antibody	Substrate	Company
TRAF1 (45D3)	SuperSignal West Pico PLUS	Thermo Scientific
TRAF3 (E8H3B)	Immobilon Forte	Millipore
c-IAP2(58C7)	Immobilon Forte	Millipore
Phospho-IκBα (Ser32) (14D4)	Immobilon Forte	Millipore
Phospho-NF-κB p65 (Ser 536) (93H1)	Immobilon Forte	Millipore
IκBα (L35A5)	SuperSignal West Pico PLUS	Thermo Scientific
Anti-Ubiquitin, Lys63 Specific (Apu3)	Immobilon Forte	Millipore

β - actin (BA3R)	SuperSignal West Pico PLUS	Thermo Scientific

Table 1. List of substrates for immunoblotting

3.7 Real-time polymerase chain reaction

a) RNA extraction

THP-1 cells are collected and washed as mentioned above. Cells were lysed in 1ml of Trizol reagent (ambion). 200ul of chloroform was added into each ER tube and vortexed for 10 seconds, then incubated at RT for 15 minutes. Samples were centrifuged at 12000rpm at 4°C for 15 minutes, then transferred 450ul of the clear supernatant to a new tube. 200ul of acid-phenol: chloroform(Invitrogen) was added into each tube. Each tube was vortexed for 10 seconds, incubated at RT for 3 minutes, then centrifuged at 12000rmp for 15 minutes. 400ul of the clear supernatant was transferred to a new tube, and the same portion of 100% isopropanol was added to it. Tubes were vortexed for 5 seconds and incubated at RT for 10 minutes. Samples were centrifuged at 12000rpm, and the supernatant was discarded. 1ml of 75% ethanol was added to each tube, and samples were centrifuged at 10000rpm for 5 minutes, repeating the steps once. The supernatant was discarded, and added 200ul of molecular biology grade water, 600ul of 100%

ethanol, 20ul of 3M NaoAC(Invitrogen), and 2ul of 20ng/ml glycogen (Thermo Scientific). RNA was precipitated at -80°C overnight. Samples were centrifuged at 10000rpm for 5 minutes on the following day and washed with 100ul of 70% ethanol. Discarded the supernatant and air dry RNA pellet for 10 minutes. Then solubilized the RNA with 50ul molecular biology grade water and incubated at 60°C for 10 minutes.

b) Reverse Transcription

RNA concentration was determined by Varioskan Lux Reader (Thermo Scientific). Before the reverse transcription, diluted RNA based on their concentration. Reaction conditions were listed in appendix section.

c) Real-time PCR

cDNA was diluted 1:10 by using molecular biology grade water. After diluting cDNA obtained from reverse transcription, the qPCR reaction plate was prepared. 4ul of diluted cDNA was added to 6ul of dye mix containing 0.5ul of forward and reverse primer and 5ul of SsoAdvanced Universal SYBR Green Supermix(Bio-Rad). All primers were validated in previous work from other lab members and the sequence of primers is shown in the following table:

Primer	Target Gene	Sequence

h-GAPDH For	GAPDH	TGACAACAGCCTCAAGAT
h-GAPDH Rev		GAGTCCTTCCACGATACC
h-TNFα For	TNFα	CTGACATCTGGAATCTGGA
h-TNFα Rev		GTCTCAAGGAAGTCTGGAA
h-IFNβ For	INFβ	TCAAGGACAGGATGAACTT
h-IFNβ Rev		GACATTAGCCAGGAGGTT
h-IL-1β For	IL-1β	TACATCAGCACCTCTCAAG
h-IL-1β Rev		ATTCAGCACAGGACTCTC
h-IL6 For	IL-6	TGAGAGTAGTGAGGAACAAG
h-IL6 Rev		CGCAGAATGAGATGAGTTG
h-IL12β For	IL-12β	ATACCAGTGCCATCATACA
h-IL12β Rev		CCATCTCCAGGAAGTCTT

Table 4. Primers used for real-time PCR

All the samples were loaded into 384-well plate and each sample had 3 technical replicates. Reaction conditions were listed in appendix section.

Quantification cycle (Cq) values is defined as the cycle number that fluorescent signal needed to reach a quantification threshold. The values were normalized by the $2^{-\Delta\Delta Ct}$

method. ΔCq values are the difference in Cq values from gene of interest (GOI) and reference gene (REF), and calculated by this formula:

$$\Delta Cq = Cq(GOI) - Cq(REF)$$

Next $\Delta\Delta Cq$ was calculated by following formula:

$$\Delta\Delta Cq = Cq(treated\ sample) - Cq(control\ sample\ average)$$

These values indicated the difference between the ΔCq of treated sample and control sample. Finally, the fold change of each gene was calculated by this equation:

$$Gene\ Expression\ Fold\ Change = 2^{-(\Delta\Delta Cq)}$$

3.8 IL-2 ELISA assay

Human IL-2 uncoated ELISA kit (Invitrogen) was used to quantify IL-2 protein levels in the supernatant of cells. 100ul of 250X anti-human IL-2 capture antibody was immobilized on a high protein binding 96-well plate (Greiner bio-one) and incubated overnight at 4°C. The plate was aspirated and washed three times with PBS containing 0.05% Tween on the following day. Then the plate was blocked with 200ul of 1x ELISA/ELISPOT diluent at RT for one hour and rewashed the plate for three times. The protein standard provided in the kit was used to create the standard curve of 15-1000pg/ml by 2-fold serial dilutions. 100ul of samples were added to the appropriate wells and incubated at RT for 2 hours. Next, the plate was washed five times, adding 100ul of diluted 250x detection antibody into each well and incubating at RT for one hour.

Rewash the plate for five times and add 100ul of diluted Avidin-HAR to incubate 30 minutes at RT. Repeat washing seven times, add 100ul of 1x TMB solution and incubate 15 minutes at RT. Lastly, 100ul of 1 M phosphoric acid was added to each well, and the plate was read at 450nm and 579nm. The concentration of protein was determined by Varioskan Lux Reader (Thermo Scientific).

3.9 Electroporation

Before the electroporation,

2×10^5cells/ml of Jurkat cells were incubate in RPMI-1640 media for 2-3 days to reach a density of 4×10^5. Viability of cells was determined by flow cytometry, only cells with high viability (>85%) were used for electroporation (Lonza). Cells were collected and transferred in 15ml conical tubes and centrifuged at 90xG for 10 minutes at RT. After the centrifugation, media was removed, and added 20ul of SE supplemented nucleofector buffer with 0.5ug of plasmids was on top of the cell pellet. The cell pellet was gently resuspended by a P-200 pipette and transferred to the Nucleocuvette reaction strip and zapped via 4D-Nucleofector System (Lonza). After nucleofection, cells were incubated at RT for 10 minutes and immediately transferred to prewarmed media in a 96-well plate.

3.10 Crispr/Cas9 HDR-mediated Knock-in Jurkat Cells

Synthetic sgRNA was purchased from Dharmacon and resuspended in 1x TE buffer. The sequence used for the synthesized of sgRNA is shown below:

Target Name	Sequence 5′-3′
TRAF1V203A	CATTGTTGCTGTCCTCAACA

Table 6. Sequence of sgRNA for CRISPR/Cas9 HDR-mediated knock-in gene editing

RNP complex for each electroporation well was prepared by following tables:

Component	Amount	Final Concentration
sgRNA(50μM)	3ul	150pmol
Alt-R Cas9 enzyme (62 μM)	2ul	125pmol
Total volume	5ul	

Table 7. Preparation of RNP complex

RNP complex then incubated at RT for 20 minutes. Cell culture media with and without Alt-R HDR Enhancer V2 (IDT) were prewarmed to 37°C. The final transfection mix for each electroporation well was prepared by following tables:

Component	Amount	Final Concentration
RNP complex	5 ul	

HDR donor oligo(100μM)	1.2 ul	4um
Alt-R-Cas9 electroporation enhancer(100μM)	1.2 ul	4um
Cell suspension	20ul	
PBS	2.6 ul	
Total	30 ul	

Table 8. Preparation of transfection mix

The sequence for HDR donor oligo was shown as below:

Target Name	Sequence 5′-3′
ssDNA TRAF1V203A	AAGCTGCGTGTGTTTGAGAACATTGTTGCTGCCCTCA ACAAGGAGGTGGAGGCCTCCCACCTG

Table 9. Sequence of oligo donor for repair

30ul of the final transfection mix was transferred to a 16-well Nucleocuvette module. After electroporation, 80ul of pre-warmed culture media (without HDR Enhancer) was added to each well. 50ul of resuspended cells were transferred to pre-warmed 150ul of culture media(with HDR Enhancer) in a 96-well plate. By the following day, media with HDR Enhancer was removed and replaced with fresh media without HDR Enhancer.

3.11 T7 cleavage assay

a) Genomic DNA extraction

500ul of Crispr/Cas9 treated cells was centrifuged at 1500rpm for 5 minutes and washed with 500ul of PBS. Cells were lysed by 50ul of QuickExtract DNA Extraction Solution (Biosearch). The lysate was heated in a thermal cycle by the following protocol:

Step	Temperature	Time
1	65°C	10 minutes
2	98°C	5 minutes

Table 10. Thermal cycler condition for genomic DNA extraction

100ul of molecular biology grade water was added to each sample to dilute the genomic DNA.

b) Amplification of the Target Site

To amplify the target site of the HDR-mediated knock-in cells, a PCR mixture was prepared by this table:

Reagent	Volume for 1 sample (μL)
2X KAPA2G Genotyping Mix	12.5 ul
RNase Free Water	7 ul
Forward Primer (10 mM)	0.75 ul
Reverse Primer (10 mM)	0.75 ul

Total Volume	21 ul

Table 11. Components used in target site amplification

The sequences and annealing temperature for TRAF1V203A were shown below:

Target Name	Sequence 5′-3′	Annealing Temperature
TRAF1V203A Forward	ATTGGGTGCCCCTTTGCAGGTG	55°C
TRAF1V203A Reverse	TCAAGCAAAGGAACCGAAGC	55°C

Table 12. Sequence and annealing temperature for TRAF1V203A primers

21 ul of the premix PCR mixture was added with 4ul of gDNA, the reaction conditions were listed in appendix section. Next, 3 ul of the DNA amplification products from the reaction was mixed with 10ul of molecular biology grade water and fractioned on a 2% agarose gel for 90 minutes at 70V. The PCR product was verified by a gel imager to detect a single band of the correct size at 500bp. The remaining product was stored at -20°C until the next steps.

c) Cleavage detection assay

The gDNA cleavage of target gene was assessed in the bulk-edited population of Jurkat cells using Alt-R Genome Editing Detection Kit (IDT). To form heteroduplexes for T7EI digestion, a mixture was prepared by the following table:

Component	Volume for 1 sample (μL)
PCR products	10 ul
T7EI reaction buffer (10x)	2 ul
Molecular Biology Grade water	6 ul
Total Volume	18 ul

Table 14. Components of heteroduplexes for T7EI digestion

Then the PCR products was heated and cool in a thermal cycler as follows:

Step	Temperature	Time
Denature	95°C	10 minutes
Ramp 1	95-85°C	Ramp rate -2°C/second
Ramp 2	85-25°C	Ramp rate -0.3°C/second

Table 15. Thermal cyclers conditions for T7EI digestion

Next, 18 ul of PCR heteroduplex from above reaction was added with 2ul of T7 endonuclease and incubated at 37°C for 1 hour. Lastly, 10ul of PCR reaction mixtures were fractioned on a 2% agarose gel. The PCR product was verified by a gel imager to detect the presence of cleavage parental bands.

3.12 Flow Cytometry

Cells from 96-well plate were centrifuged at 1500rpm for 5 minutes at 4°C to remove culture media. Each well was added 100ul of 1x IC fixation buffer and incubate in the darkness at RT for 30 minutes. Then buffer was aspirated and added 150ul of ice-cold 100% methanol and incubate in the darkness at 4°C overnight. On the following day, 100ul of FACS buffer (PBS -/- with 2% FBS) was added on top of each well and centrifuged at 1200rpm for 2 minutes at 4°C. Repeat the washing with 200ul FACS buffer and centrifuge the plate. In each well was added 50ul of FACS buffer with 1ul of p-ERK (Invitrogen) and p-p65 (Invitrogen) antibodies. Then the plate was incubated in the darkness at 4°C for 25 minutes. Once complete, 200ul of FACS buffer was added on top to each well and centrifuged at 1200rpm for 2 minutes at 4°C and repeat the washing step one more time. Finally, resuspend the cells in 200ul of FACS buffer and loaded into the Attune NxT Flow Cytometer (ThermoFisher Scientific).

Target	Fluorphore	Laser	Channel
p-ERK	Alexa Fluor 488	Blue 488nm	530/30
p-p65	eFluor 660	Red 637nm	670/14

Table 16. Fluorescence information for antibodies used in flow cytometry

The results were analyzed by flow jo and gating strategy for flow cytometry was shown below:

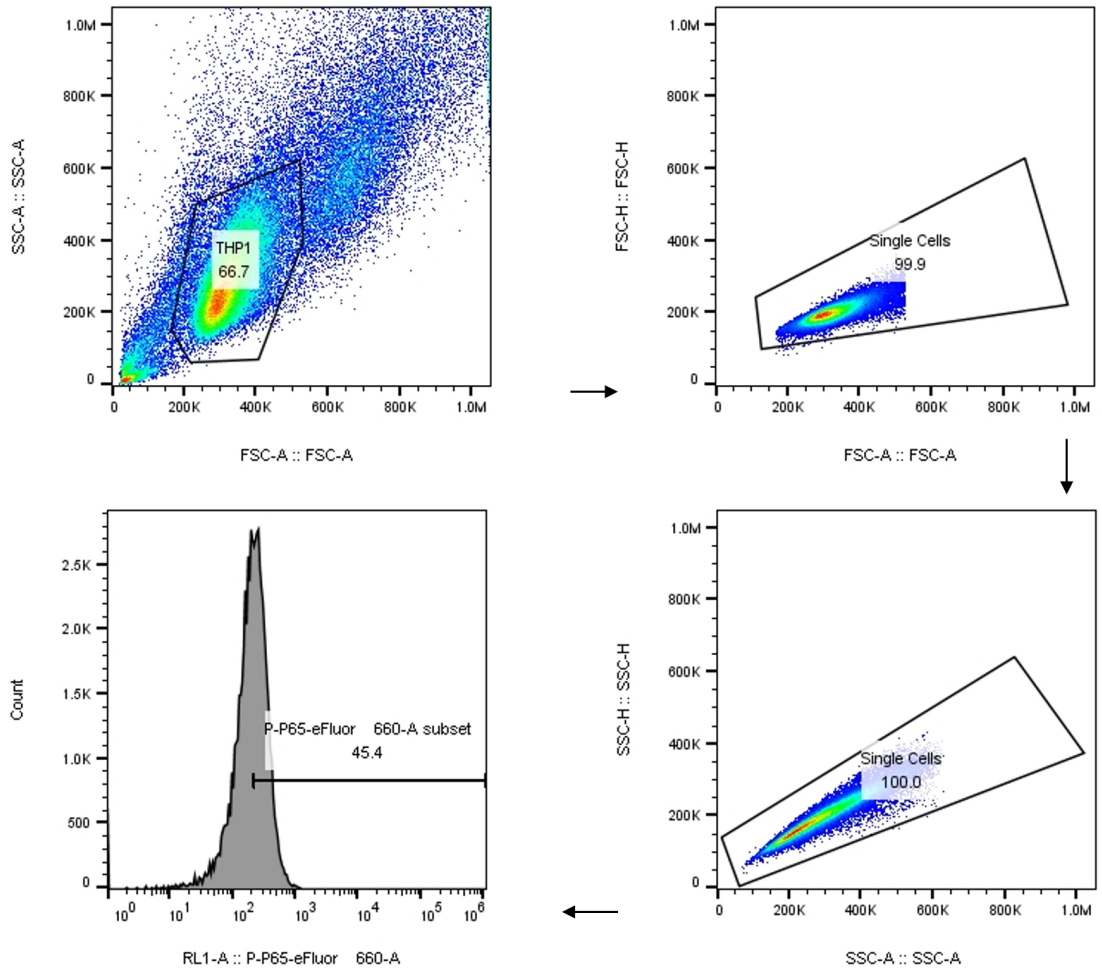

Figure 4. Gating strategy for flow cytometry analysis of phosphorylation status. Cells were loaded into the flow cytometer once the cells were fixed, stained, and washed with FACS buffer. The unstained sample was used to ensure most of the cells were in the middle of each plot. The gating strategy was used to exclude debris, doublets, and dead cells from analysis. This strategy is representative of what was used in all flow cytometry experiments.

3.13 Statistical Analysis

Results were compared by RM one-way ANOVA with the Geisser-Greenhouse correction, two-way ANOVA with the Geisser-Greenhouse correction, Šidák's multiple comparison

test and Dunnett's multiple comparison test by GraphPad Prism 9.0. A $p<0.05$, $p<0.01$, $p<0.001$, and $p<0.0001$ were considered as significant. Data are reported as mean ± SEM.

Chapter 4 Results

4.1 TRAF1 V203A mutation abrogates interaction between c-IAP2

The first step in this project is to examine the effects of TRAF1V203A mutated THP-1 cell lines on interacting with the c-IAP2 protein. Previously, students from our lab created this cell line via CRISPR/Cas9 HDR-mediated knock-in gene editing technology. Since TRAF1 and c-IAP2 cannot be detected at basal levels in THP-1 cell lines, we treated wild-type THP-1 cells and TRAF1V203A THP-1 cells with or without 100 ng/ml of LPS for 24 h. Lysates were then co-immunoprecipitated with an anti-TRAF1-specific antibody(1F3) and immunoblotted for TRAF1 and c-IAP2 (Figure 5). More c-IAP2 was pulled down in wild-type THP-1 compared to the TRAF1V203A mutation. Based on this result, we

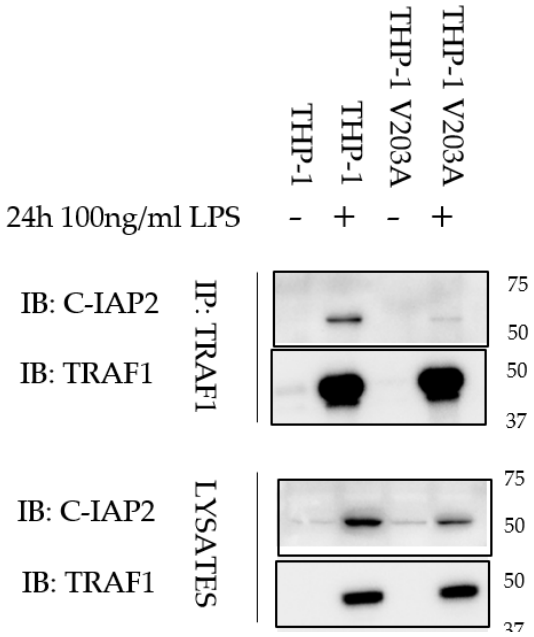

Figure 5. Effects of TRAF1V203A on c-IAP2. Co-Immunoprecipitation (CO-IP) of TRAF1 from lysates of THP-1 and THP-1 V203A cells, followed by immunoblotting (IB) with c-IAP2 and TRAF1 specific antibodies and anti-rabbit-horseradish peroxidase. The data shown are representative of three independent experiments.

confirm that within the TRAF1V203A mutation, the interaction between TRAF1 and c-IAP2 diminishes.

To further confirm this result, we repeated the CO-IP experiment but only used decreased cell lysates from wild-type THP-1 cells. Instead of immunoprecipitating with a full amount (950 ul) of cell lysate, we used half the amount (475 ul) and a quarter of the cell lysate (237.5 ul) from wild-type THP-1 cells to repeat the co-immunoprecipitation. Surprisingly, the result in Figure 6 shows that even though the amount of cell lysate used for co-immunoprecipitation was decreased, wild-type THP-1 cells could still pull down more c-IAP2 protein compared to TRAF1V203A THP-1 cells. This result confirms that the interaction with c-IAP2 is significantly lost in TRAF1V203A mutated THP-1 cells.

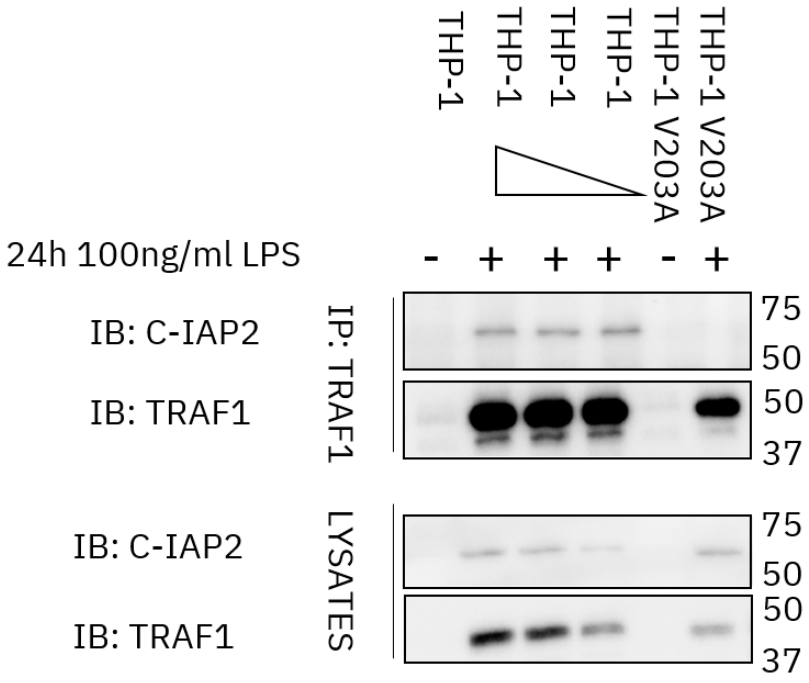

Figure 6. Comparison of interaction on c-IAP2 when decreased cell lysate from WT THP-1 for CO-IP. Co-Immunoprecipitation (CO-IP) of TRAF1 from lysates of THP-1 and THP-1 V203A cells, followed by immunoblotting (IB) with c-IAP2 and TRAF1 specific antibodies and anti-rabbit-horseradish peroxidase. The data shown are representative of three independent experiments.

To eliminate any effects of non-specific binding in our results, we further co-immunoprecipitated lysates with an IgG control antibody and immunoblotted for TRAF1 and c-IAP2 (Figure 7). However, the IgG isotype control did not pull down any band

when immunoblotted for either TRAF1 or c-IAP2 antibody, which indicated that no non-specific binding was present in our results.

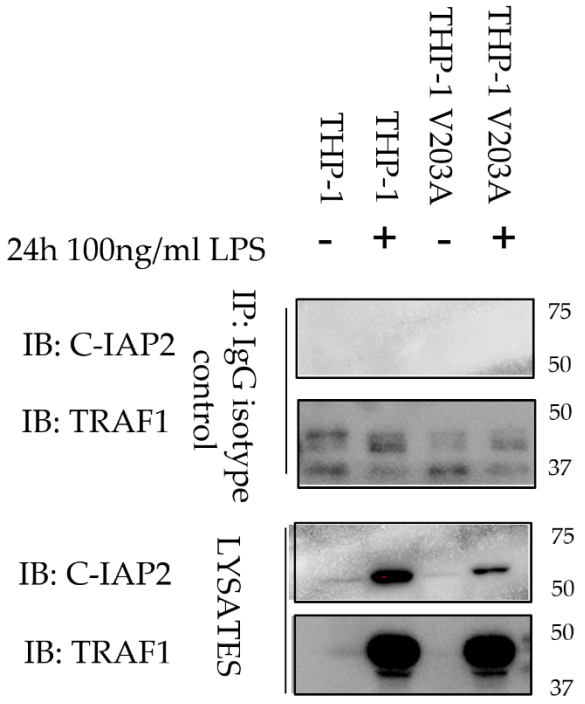

Figure 7. Eliminated the possibility of non-specific binding Co-Immunoprecipitation (CO-IP) of TRAF1 from lysates of THP-1 and THP-1 V203A cells, followed by immunoblotting (IB) with c-IAP2 and TRAF1 specific antibodies and anti-rabbit-horseradish peroxidase. The data shown are representative of three independent experiments.

All the results suggest that CRISPR/Cas9 HDR-mediated knock-in of TRAF1V203A THP-1 cells abolishes the interaction with c-IAP2, but this interaction remains intact in WT THP-1 cells.

4.2 Effect of TRAF1V203A in TLRs and TNFR1

The next goal of the project is to assess whether the TRAF1V203A mutation affects the downstream pathway. Previous students have already confirmed that the TRAF1V203A only affects the interaction with TRAF1 and c-IAP2, while maintaining its interaction with TRAF2 and LUBAC. This mutation allows us to only examine NF-κB activation in TLRs or TNFR1 downstream pathways.

To activate the TNFR1 and TLRs pathways separately, we stimulated WT THP-1 and TRAF1V203A THP-1 cells with human TNF-α or LPS, respectively. To avoid results caused by coincidence, we selected two colonies that only acquired the TRAV1V203A mutation. In the TNFR1 pathway stimulation, cells were stimulated with 100 ng/ml of human TNF-α for 15, 30, and 60 minutes. Figure 7 showed that both clones of TRAF1V203A cells expressed more total IκB-α than WT THP-1 cells, which indicated that less IκB-α was phosphorylated. At the same time, TRAF1V203A cells also expressed more phospho-IκB-α than WT THP-1 cells. However, the expression of phopho-p65 (a subunit of NF-κB) decreased in two clones of TRAF1V203A THP-1 cells at 15 and 30 minutes. IκB-α expression is only present without stimulation and starts degradation once stimulated with TNF-α. These results suggest that TNF-α induced NF-κB activation is downregulated in TRAF1V203A mutated THP-1 cells.

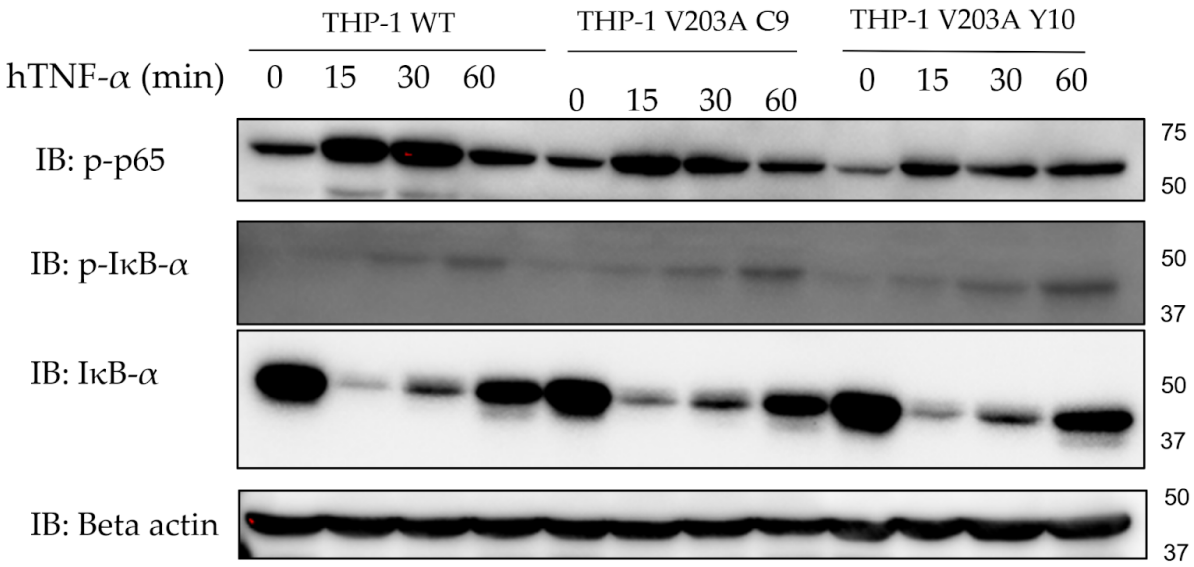

Figure 8. TNF-α induced NF-κB activation in WT THP-1 and TRAF1V203A THP-1 cells. Both cells were stimulated with 100ng/ml of human TNF-α for 15, 30 and 60 minutes. Cells were lysed and the whole cell lysates were obtained. Followed by immunoblotting with phospho-p65 (p-p65), phospho-IκB-α (p-IκB-α), total IκB-α (IκB-α) and beta-actin as the loading control. The data shown are representative of three independent experiments.

To examine NF-κB activation in the TLRs pathways, we treated WT THP-1 and two clones of TRAF1V203A mutated THP-1 cells with 100 ng/ml of LPS. Surprisingly, TRAF1V203A THP-1 cells expressed more total IκB-α compared to WT THP-1 cells (Figure 9). Compared to WT THP-1 cells, the expression of phospho-p65 also decreased in TRAF1V203A THP-1 cells, especially in the Y10 clone. Combining both results, we find that TRAF1V203A mutated THP-1 cells downregulate both TNF-α induced and LPS induced NF-κB activation.

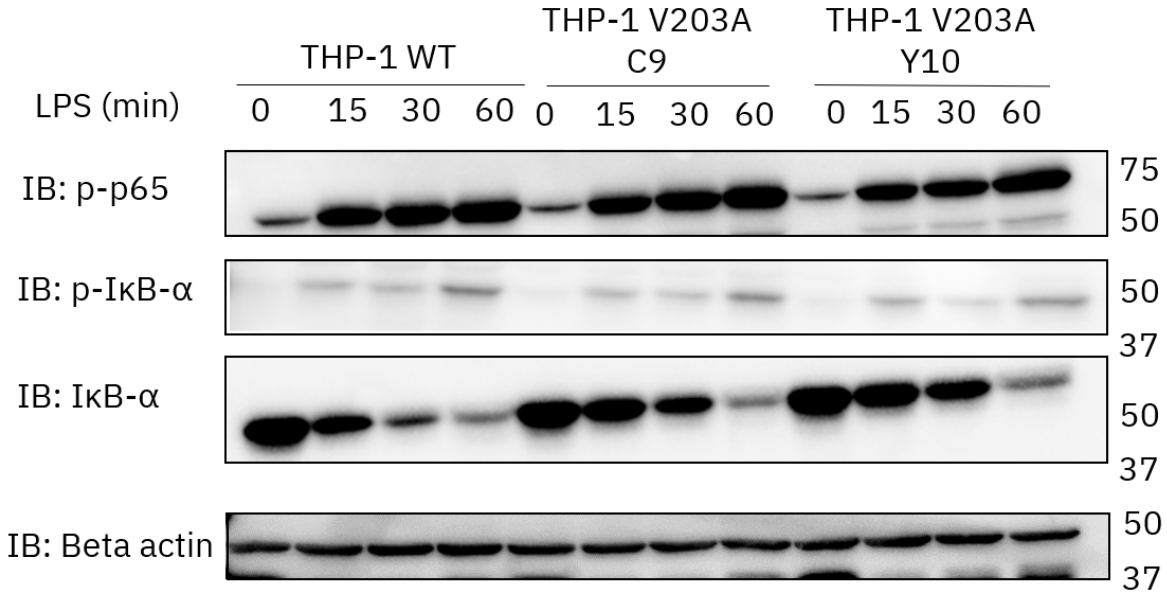

Figure 9. LPS induced NF-κB activation in WT THP-1 and TRAF1V203A THP-1 cells. Both cells were stimulated with 100ng/ml of LPS for 15, 30 and 60 minutes. Cells were lysed and the whole cell lysates were obtained. Followed by immunoblotting with phospho-p65 (p-p65), phospho-IκB-α (p-IκB-α), total IκB-α (IκB-α) and beta-actin. The data shown are representative of three independent experiments.

4.3 Decrease of K63 linked ubiquitination in TRAF1V203A

A graduate student from our lab found that inflammasome activation was inhibited in TRAF1V203A cells. Another research also pointed out that c-IAP2 and TRAF2 interact with caspase-1 and direct its K63 ubiquitination [61]. To activate K63-linked ubiquitination, we primed WT THP-1 and TRAF1V203A THP-1 cells with LPS for 24 h and then activated them with nigericin for 2, 10, or 25 minutes, and then performed immunoprecipitation for caspase-1. Ubiquitinated protein could form a smear on gel, indicating the level of ubiquitination modification. This result (Figure 10) found that K63 ubiquitination had a stronger smear in WT THP-1 cells compared to TRAF1V203A cells. We confirm that K63 ubiquitination decreases in the TRAF1V203A mutation, which also support previous findings from our lab.

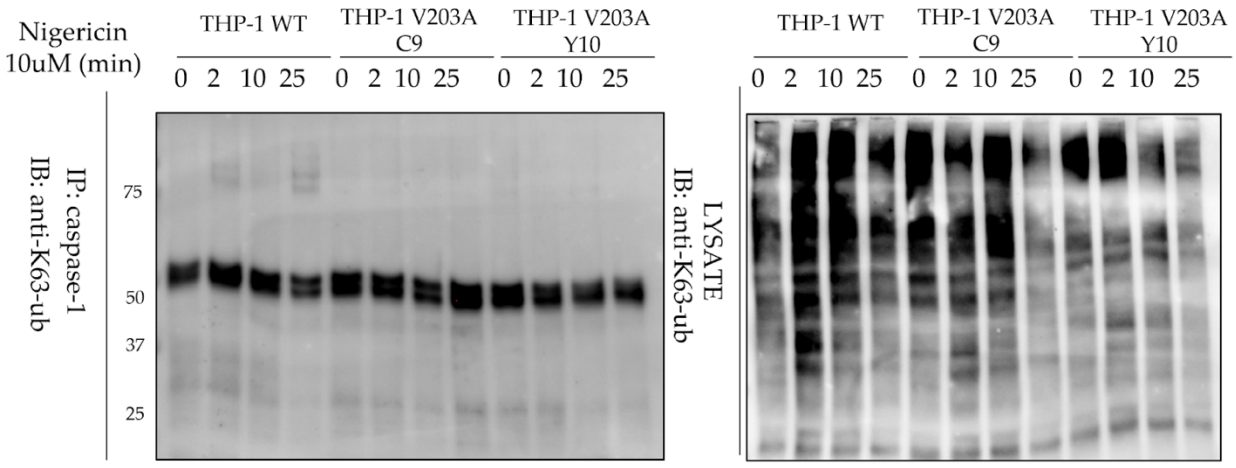

Figure 10. K63-linked ubiquitination in WT THP-1 and TRAF1V203A THP-1 cells. Both cells were primed with 100ng/ml of LPS for 24 hours and stimulated with nigericin for 2, 10 and 25 minutes. cells were scraped and lysed to obtain the whole cell lysate. Immunoprecipitation of endogenous caspase-1 was performed, and immunoblotting for K63 ubiquitin. The data are representative of two independent experiments.

4.4 Change of Gene Expression in TRAF1V203A mutation

Another way to measure NF-κB activation in the TRAF1V203A mutation is by real-time PCR. This allowed us to assess the expression of various genes responsible for inflammation and NF-κB activation. WT THP-1 and TRAF1V203A THP-1 cells were treated with human TNF-α or LPS for 1, 3 or 6 hours. After treatment, the cells were lysed and RNA was extracted. The cDNA was reverse transcribed from the RNA and amplified with different primers to measure gene expression. GAPDH, human TNF-α, human INFβ, human IL-1β, human IL-6 and human IL-12β were analysed. Upon completion of the reaction, the Cq values of each gene of interest were normalised to the housekeeping gene GAPDH. Gene expression results were expressed as fold change relative to the unstimulated control. Figure 10 shows that the expression of the pro-inflammatory cytokines IL-1β and IL-6 was significantly higher in WT THP-1 cells compared to TRAF1V203A, regardless of whether this was activated downstream of TLRs or TNFR1. Interestingly, the expression of another pro-inflammatory gene, TNF-α, was higher in both clones of TRAF1V203A THP-1 cells, especially upon LPS treatment. The TRAF1V203A Y10 clone increased 73.46-fold compared to 14.22-fold in WT THP-1 cells. However, the fold change for IL-12β was significantly greater in both WT THP-1 and one of the TRAF1V203A clones (Y10) compared to another TRAF1V203A clone. Our results did not show a significant difference in fold change for INFβ in human TNF-α stimulated cells. However, the expression of INFβ was significantly higher in

WT THP-1 cells when treated with LPS. The evidence from the downregulation of IL-1β and IL-6 supports our hypothesis that NF-κB activation is reduced in TRAF1V203A mutated THP-1 cells.

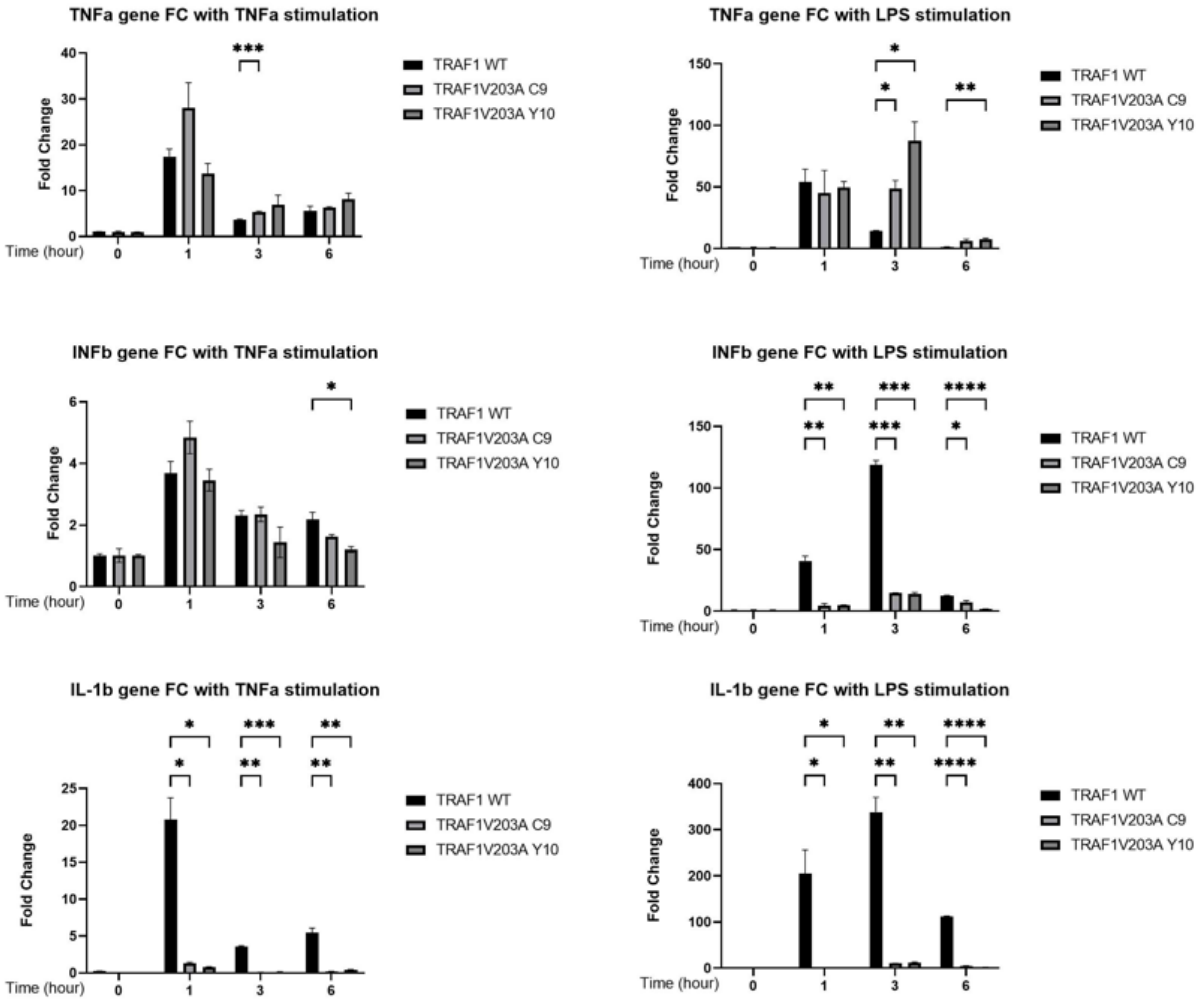

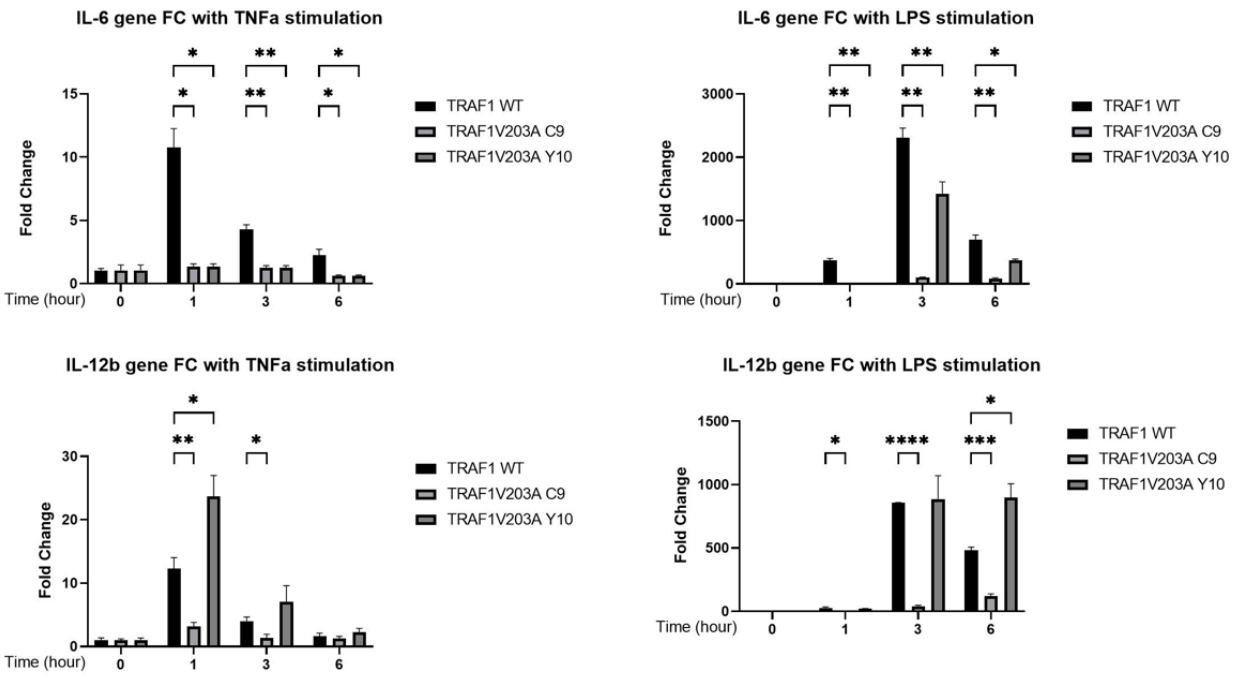

*Figure 11. Real-time PCR results indicating change of gene expression in WT THP-1 and TRAF1V203A mutated THP-1 cells. cDNA created from RNA extracted from WT THP-1 and TRAF1V203A mutated THP-1 cells that treated with 100ng/ml of LPS or TNF-α for 1, 3 or 6 hours. GAPDH, human TNF-α, human INFβ, human, IL-1**β**, human IL-6 and human IL-12**β** were analysed. Bars indicate fold change normalized to housekeeping gene GAPDH with respect to the non-stimulated control. Values are means and standard deviations. The results include data from four independent experiments. *=p< 0.05, **=p<0.01, ***=p<0.001, ****=p<0.0001 by two-way ANOVA.*

4.5 Flow Cytometry analysis for protein phosphorylation status in TRAF1V203A

Since the results of real-time PCR differed from our findings in protein expression, another way to measure NF-κB activation would be to analyse protein phosphorylation status by flow cytometry. Phospho-ERK1/2 and phospho-p65 were used to measure NF-κB activation in this assay. The results are shown in Figure 11. The bars indicate the fold change with respect to the unstimulated control. Using flow cytometry, we found no difference in the phosphorylation level of p65 between WT THP-1 and TRAF1V203A mutant cells when treated with TNF-α. Furthermore, there was a slight difference in p-ERK1/2 between WT THP-1 and TRAF1V203A mutant cells, but the overall phosphorylation trend was about the same in both cell lines. Contrary to our expectations, the phosphorylation levels of ERK1/2 were about 3-fold higher in WT THP-1 than in TRAF1V203A (C9, 2.6-fold; Y10 3-fold). A similar result was found for p-p65, which increased 3.8-fold in WT THP-1, but only 1.9-fold in C9 and 2.9-fold in Y10.

These results suggest that the phosphorylation levels of ERK1/2 and p65 decrease in the TRAF1V203A mutation when the TLR pathway is activated.

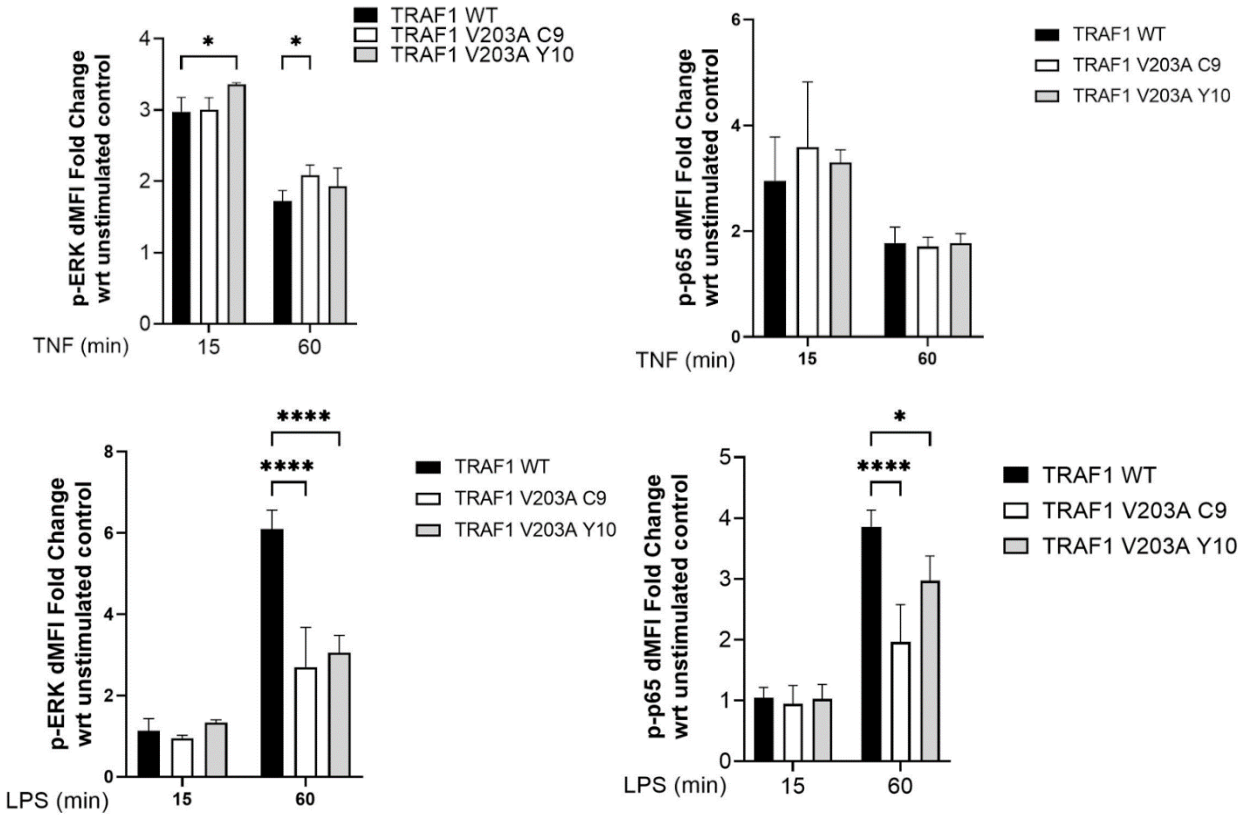

*Figure 12. Flow cytometry analysis of protein phosphorylation status in WT THP-1 and TRAF1V203A THP-1 cells Cells were treated with 100ng/ml of LPS or TNF-α for 15 and 60 minutes. Cells were stained with p-ERK1/2 and p-p65 to measure phosphorylation level. Mean channel fluorescence intensity (MFI) derived from fluorescence histogram was used to measure the level of phosphorylation of ERK1/2 and p65. Delta MFI (dMFI) was calculated as a subtraction and recorded as the MFI of the p-ERK1/2 or p-p65 antibody minus the MFI of the fluorescence minus one (FMO) control. Bars represented fold change normalized to non-stimulated control. Values are means and standard deviations. The results include data from six independent experiments. *=p< 0.05, **=p<0.01, ***=p<0.001, ****=p<0.0001 by two-way ANOVA.*

4.6 TRAF1V203A prevents TRAF3 degradation

The results from flow cytometry were completely different from what we found from immunoblotting. Another possible explanation is that TRAF3 degradation in TLR signalling promotes the expression of pro-inflammatory cytokines. To test our hypothesis, we treated WT THP-1 and TRAF1V203A cells with LPS for 15, 30 and 60 minutes. We then immunoblotted for TRAF3 to measure degradation levels. After activation, TRAF3 showed degradation at 15 minutes in both WT THP-1 and TRAF1V203A (Figure 12). To better compare the intensity between bands, we quantified the protein bands. The results are shown on the right-hand side of this figure. It clearly shows that TRAF1V203A prevents TRAF3 degeneration compared to WT THP-1 at 30 and 60 minutes. This result could be a possible reason why we saw the downregulation of the pro-inflammatory gene and the decreased phosphorylation status of ERK1/2 and p-65 in the previous experiment..

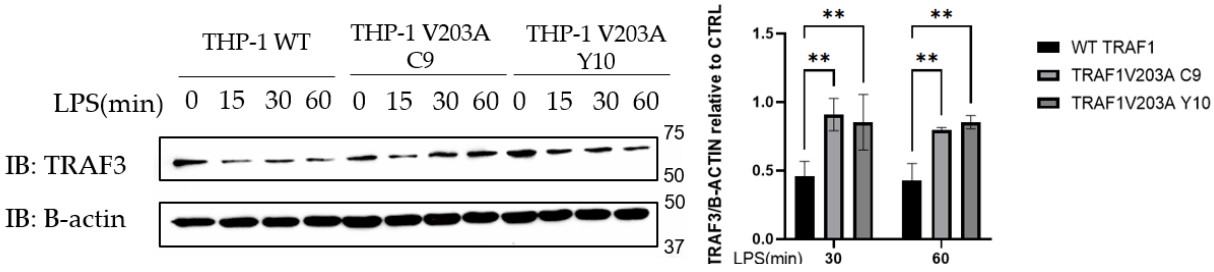

*Figure 13. TRAF1V203A prevents TRAF3 degradation. WT THP-1 and TRAF1V203A mutated THP-1 were treated with 100ng/ml of LPS for 15, 30 and 60 minutes. Followed by immunoblotting with TRAF3 and beta actin specific antibodies. The intensity of bands was quantified from ImageLab. The quantification reflected the relative amounts as the ratio of each protein band relative to loading control. Bars represented fold change normalized to non-stimulated control. Values are means and standard deviations. The immunoblotting result is representative of three independent experiments. The chart includes data from three independent experiments. *=p< 0.05, **=p<0.01, ***=p<0.001 by two-way ANOVA.*

4.7 Overexpression of TRAF1V203A in T cell

As an immunoregulatory cytokine, IL-2 promotes lymphocyte survival and differentiation. To further investigate how TRAF1V203A affects the TNFR signalling pathway in lymphocytes, we overexpressed Jurkat T cells with empty c-flag, WT TRAF1(TRAF1-FL) and TRAF1V203A plasmids by electroporation. To confirm that all plasmids were successfully electroporated into Jurkat T cells, we also performed a western blot, as shown in Figure 14.

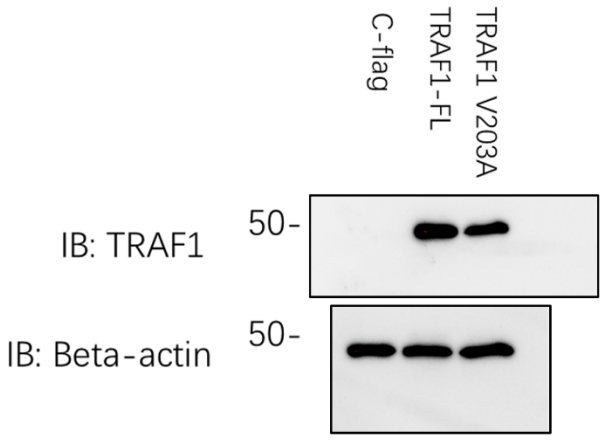

Figure 14. Confirmation of Jurkat T cells overexpression with TRAF1-FL or TRAF1V203A. An overexpression in Jurkat T cells with 0.5 ug of c-flag, TRAF1-FL and TRAF1V203A plasmids. Plasmids were introduced by electroporation then immunoblotted with TRAF1 and beta actin specific antibody. Experiment was performed one time.

Since T cells need a co-stimulatory signal to activate, we used anti-CD3 antibody and anti-4-1BB antibody as two signals to activate them and then analysed them for IL-2 secretion after 24 hours. Our results in Figure 15 shows that T cells secreted more IL-2

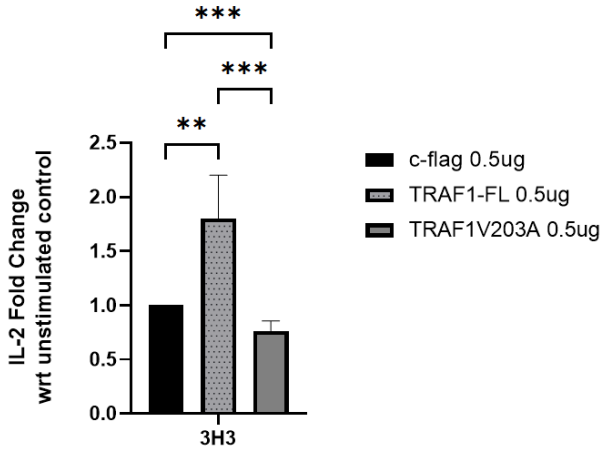

*Figure 15. IL-2 ELISA results from Jurkat cells supernatant that overexpressed with TRAF1-FL or TRAF1V203A. After electroporated cells were incubated anti-CD3(1μg/mL) and anti-4-1BB antibody(10μg/mL) overnight. Supernatant was collected and added to a coated IL-2 ELISA plate. Fluorescence was measured and used to determine the concentration of secreted IL-2 in each sample. Bars represented fold change normalized to non-stimulated control. Values are means and standard deviations. The results includes data from three independent experiments. *=p< 0.05, **=p<0.01, ***=p<0.001 by one-way ANOVA.*

when overexpressed with WT TRAF1. However, the IL-2 levels in TRAF1V203A were lower than WT TRAF1 and the empty plasmid control. These results suggest that IL-2 production and NF-κB activation of T cells are decreased with the TRAF1V203A mutation.

4.8 Genomic Cleavage of TRAF1V203A site targeted by sgRNA in Jurkat T Cells

To study the physiological response of the TRAF1V203A mutation in lymphocytes, we generated TRAF1V203A mutated T cells using CRISPR/Cas9. To test whether our CRISPR-edited bulk was successfully targeted by sgRNA, a T7EI genomic cleavage detection assay was performed. We extracted genomic DNA from edited Jurkat cells and amplified the specific double-strand break loci by PCR. The PCR product was then reannealed to allow a potential duplex to form between the wild-type and CRISPR-mutated DNA. Finally, the annealed PCR product was digested with a detection enzyme to check for mismatches in the genomic DNA. We used TRAF1V203A mutant THP-1 as a positive control and Figure 15 shows a prenatal band of TRAF1V203A at 498bp. We also saw two cleaved bands (190bp and 308bp) in the Jurkat CRISPR-edited

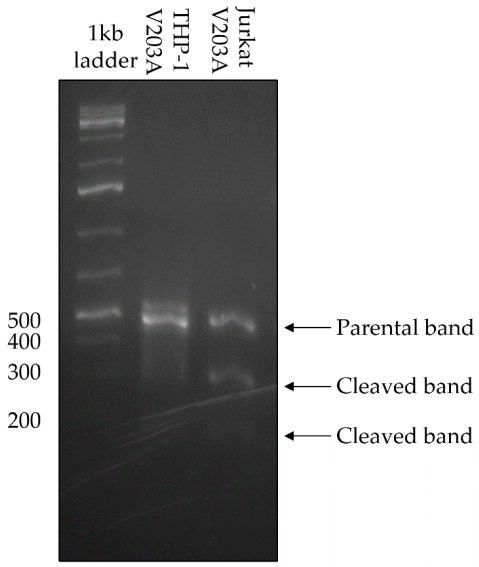

Figure 15. Gel image of CRISPR/Cas9 HDR-mediated knock-in bulk cells. Gel image of genome editing detection assay for Jurkat cells. Samples were amplified with TRAF1V203A targeting primers. Samples were separated on a 2% agarose gel.

bulk population. The presence of two cleaved fragments indicate that TRAF1V203A has been successfully targeted by the sgRNA.

4.9 Sequencing Chromatographs for TRAF1 V203A Locus

After we had confirmed that CRISPR had successfully edited our Jurkat T bulk population, single cell clones were grown from the bulk population. To verify the V203A mutation, genomic DNA was extracted from each single cell clone and amplified using TRAF1V203A primers. The PCR products were then purified and sent to The Centre for Applied Genomics (TCAG) DNA/sequencing facility. The V203A site was encoded as GTC (valine) in wild-type TRAF1. To create a V203A mutation in TRAF1, we need to mutate this site to alanine (GCC). The chromatograms of the black, red and blue peaks in Figure 15 indicate G, T and C nitrogen bases respectively.

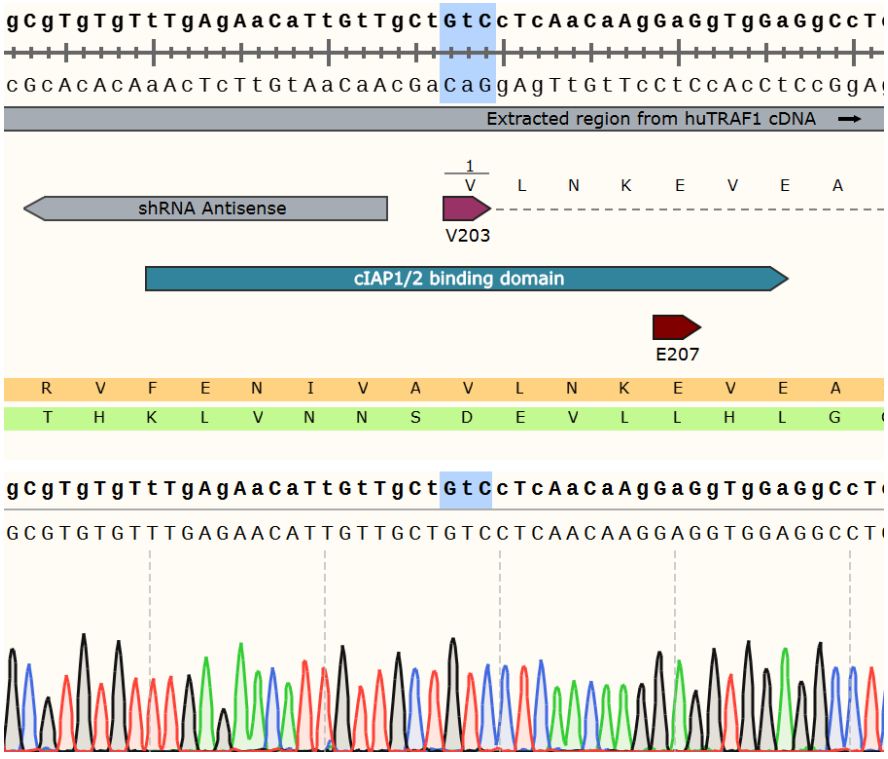

Figure 16. Sequencing chromatographs for WT TRAF1 in Jurkat cells.Genomic DNA were extract and amplified V203A target site and sequenced. Black, red, and blue peaks indicated G, T and C nitrogenous base respectively.

We then used the Guide-It Knock-in Screening Kit to perform an enzymatic assay by real-time PCR. This assay allows us to select potential homozygous TRAF1V203A knock-in from single cell colonies. Green fluorescence indicates homozygous with the V203A mutation, red fluorescence indicates homozygous WT TRAF1 and the combination of red and green indicates heterozygous. After screening hundreds of additional single cell colonies, in Figure 17 we identified six single cell colonies that

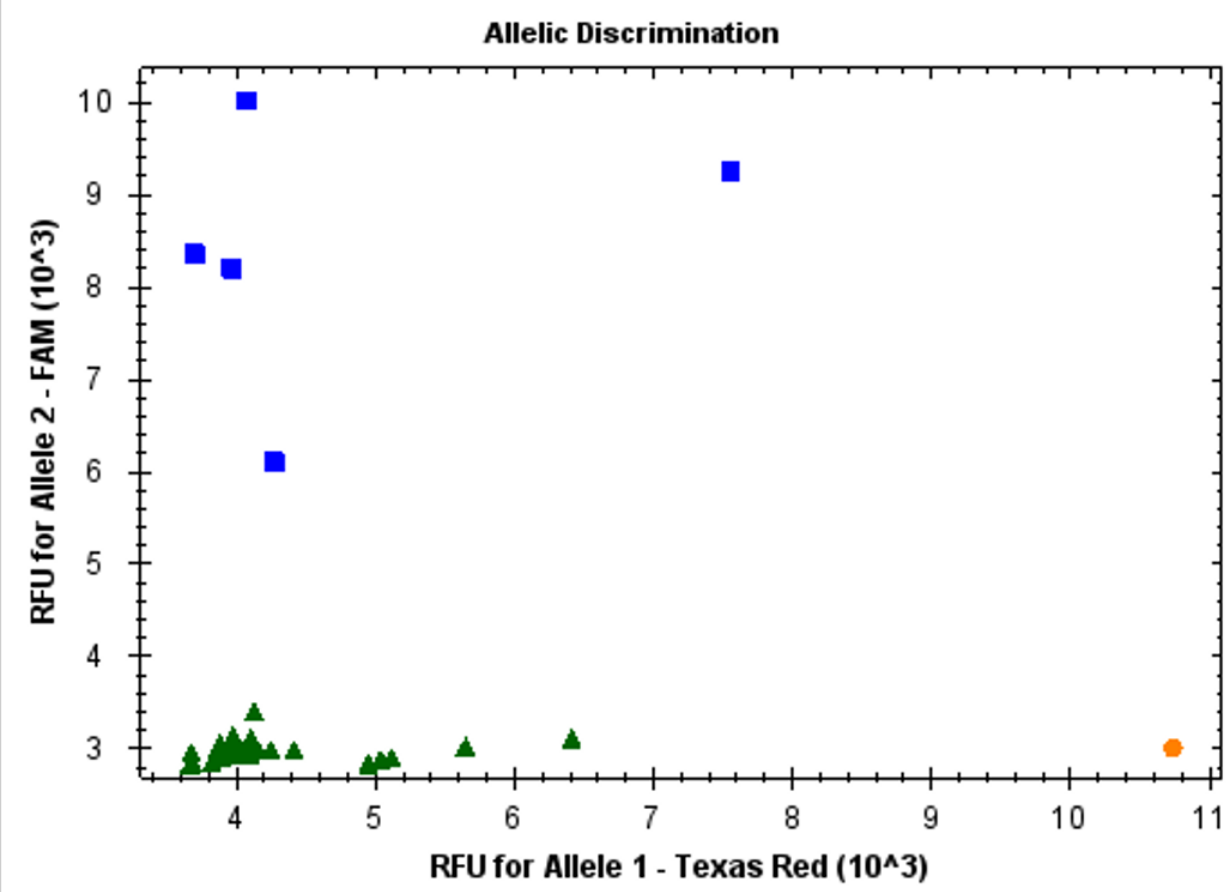

Figure 17. Allelic discrimination of CRISPR/Cas9 HDR-mediated knock-in of TRAF1V203A mutation in Jurkat cells.Allelic discrimination was used to detect single base pair difference of target sequences. Blue squares indicated homozygous (with green fluorescence) of TRAF1V203A mutation, orange circles indicated WT TRAF1, green triangles indicted heterozygous. RFU stands for relative fluorescent unite.

showed only green fluorescence and were considered to be potential homozygous TRAF1V203A mutant Jurkat cells. These potentially homozygous cells were sent for further sequencing.

Unfortunately, the result in Figure 18 shows that none of them contained the homozygous TRAF1V203A mutation without any additional errors or substitutions, even though CRISPR/Cas9 successfully targeted the site.

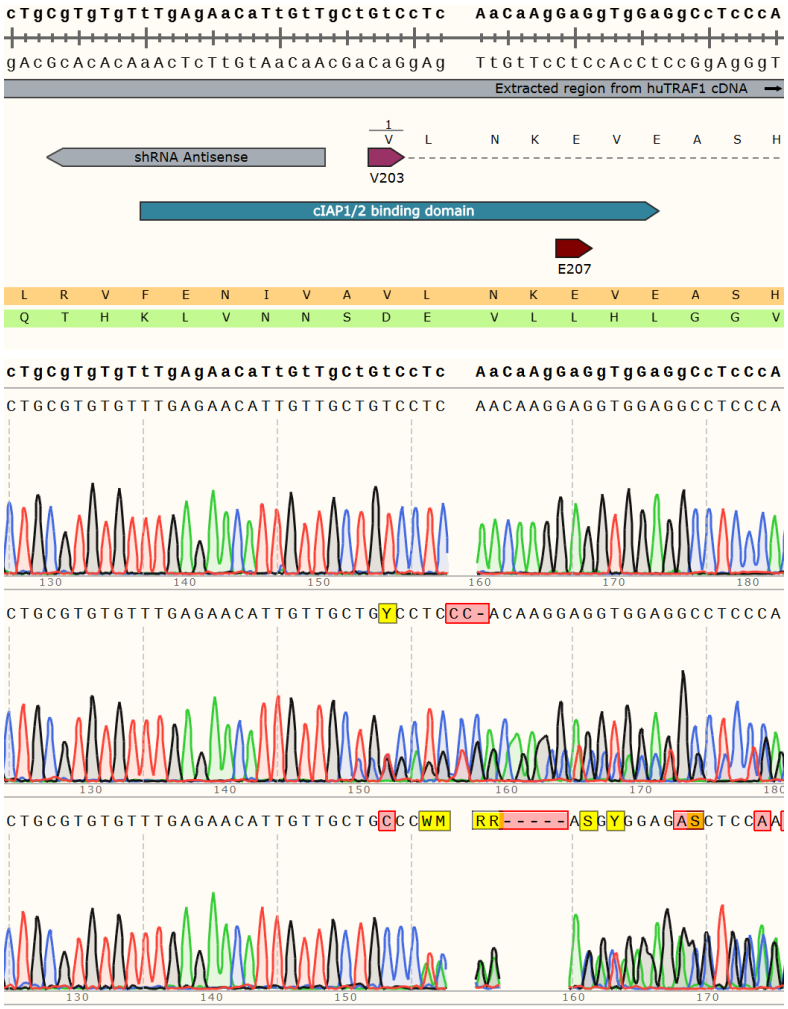

Figure 18 Sequencing chromatographs for TRAF1V203A mutation in Jurkat cells. *Genomic DNA were extract and amplified V203A target site and sequenced. WT TRAF1 was presented at the top of the figure. No clean point mutation at TRAF1V203A region was found. The data shown are representative of many sequencing results.*

Chapter 5 Discussion

Some studies have reported that TRAF1 downregulates TLR-mediated NF-κB activation by inhibiting LUBAC and blocking linear ubiquitin chains. In contrast, others have shown that TRAF1 enhances TNFR-mediated NF-κB activation by recruiting c-IAP2 [7,11]. Results from other studies also suggest that TRAF1 plays an essential role in the immune response. However, an overreaction to these pathways can lead to the development of autoimmune diseases such as rheumatoid arthritis [62]. Published work from our laboratory has already shown that reduced TRAF1 levels are associated with an increased risk of developing rheumatoid arthritis [33]. Previous work on TRAF1 has also shown that TRAF1-deficient mice (TRAF1-/-) have increased NF-κB activation and T cell proliferation [21]. Unpublished work from our laboratory also supports that the absence of TRAF1 promotes more inflammation in the synovium of mice. Therefore, blocking TRAF1 completely is not the best option to study its function and mechanism. A previous student in our lab found that mutation of the residues valine 203 to alanine can prevent the interaction between TRAF1 and c-IAP2 but retain the ability to interact with both TRAF2 and HOIL-1. This mutation allows us to study the role of TRAF1 in TLR or TNF receptors separately. Another student in our lab generated TRAF1V203A mutant THP-1 human monocytes using CRISPR/Cas9 gene editing technology. With these cell lines, we can study their role in regulating NF-κB activation. To start with, we need to create a functional assay to test the effect of TRAF1V203A mutant THP-1 cells.

Using co-immunoprecipitation, we confirmed that the interaction between c-IAP2 and TRAF1 is reduced in TRAF1V203A mutant compared to WT TRAF1. To study NF-κB activation downstream of TLRs and TNFRs, we stimulated TRAF1V203A cells with human TNF-α or LPS. Through these experiments, we found that NF-κB activation was significantly reduced when TRAF1V203A mutant THP-1 cells were treated with human TNF-α. This change was due to decreased phosphorylation of its inhibitor IκBα in mutant THP-1 cells. However, we also found the same effects when they were treated with LPS. Since our Western blot results are not quantitative, to quantify NF-κB activation downstream of TNFRs and TLRs, we further examined the phosphorylation status of the protein by flow cytometry. Surprisingly, we saw no difference in the change in phosphorylation levels of p65 and ERK1/2 with TNF-α stimulation. However, upon LPS stimulation, the phosphorylation level of p65 and ERK1/2 was significantly lower in TRAF1V203A mutant THP-1 cells. A study by Mahoney et al. found that c-IPA1 and c-IPA2 can facilitate TNFα-mediated NF-κB activation [54]. As c-IAP1 and c-IAP2 are redundant in TNFα-mediated signalling, the inhibition of interaction with c-IAP2 in this case could be compensated by c-IAP1 [64]. Taken together, these findings may explain why we did not see effects on gene expression and phosphorylation levels when we stimulated TRAF1V203A cells with TNFα.

On the other hand, the study by Tseng suggested that degradative TRAF3 ubiquitination in TLR signalling is essential for the activation of mitogen-activated

protein kinases (MAPKs) and inflammatory cytokine production [65]. These results may support the decrease in phospho-ERK1/2 in TRAF1V203A mutant cells when stimulated with LPS. We also measured TRAF3 degradation after LPS stimulation to further test our hypothesis. As we predicted, TRAF1V203A prevented TRAF3 degradation and reduced ERK1/2 phosphorylation.

We also analysed the gene expression of pro-inflammatory cytokines in TRAF1V203A mutant THP-1 cells. Analysis of real-time PCR data shows significantly lower expression of IL-1β and IL-6 in TRAF1V203A mutant cells under both TNF-α and LPS stimulation. However, the expression of IL-12β was upregulated in one of the TRAF1V203A mutant clones compared to WT TRAF1. Interestingly, the expression of INFβ showed significant downregulation upon LPS stimulation in TRAF1V203A mutation compared to WT TRAF1. Since INFβ production indicates the activation of the TRIF-dependent TLR pathway, we were surprised to find that the TRAF1V203A mutation also somehow downregulates the IRFs.

The next component of this project was to investigate the ability to complete K63 ubiquitination of caspase-1. One of our lab members showed that inflammation activation was reduced in TRAF1V203A mutant THP-1 cells, which could be supported by a study showing that c-IAP1/2 is essential for caspase-1 activation [61]. We found that K63-linked ubiquitination was lower in TRAF1V203A mutated THP-1 compared to

WT THP-1. Our results confirmed that interaction with c-IAP2 is necessary for caspase-1 activation.

Activation of the 4-1BB pathway leads to cytokine production and T cell proliferation through activation of the NF-κB pathway [14]. To investigate the effect of the TRAF1V203A mutation on the adaptive immune response, we overexpressed TRAF1V203A in Jurkat T cells and measured IL-2 secretion by ELISA. Our results indicated that the TRAF1V203A mutation secreted less IL-2 cytokine compared to WT TRAF1. This suggested that the reduced NF-κB activation in TRAF1V203A overexpressed T cells was indirect. To address this, we generated TRAF1V203A knock-in Jurkat cells using the CRISPR/Cas9 method. We introduced the Cas9/sgRNA-RNP complex and donor ssDNA into Jurkat cells by electroporation. Unfortunately, although we confirmed that CRISPR/Cas9 successfully targeted the bulk of TRAF1V203A Jurkat cells, we were unable to isolate a heterozygous clone of TRAF1V203A without errors or other mutations.

Chapter 6 Future Directions

Although we used many assays to measure NF-κB activation in TRAF1V203A, some questions remained. We can use immunofluorescence to identify phosphorylated proteins by microscopy. More research is also needed on c-IAP1 and c-IAP2. To understand more about the compensatory effects of c-IAP1/2, we can knock down c-IAP1 in TRAF1V203A mutant THP-1 cells with siRNA. The next goal of this study is to generate TRAF1V203A knock-in Jurkat T cells without additional errors or substitutions. These cells will allow us to study NF-κB activation from the adaptive immune side. We can use flow cytometry and monitor the proliferation rate of the T cells using the carboxyfluorescein diacetate succinimidyl ester (CFSE) method. After studying the effects of TRAF1V203A in both monocytes and lymphocytes, we can transfer our work to the TRAF1V203A mutant mouse and observe how it affects the progression of inflammation and the production of pro-inflammatory cytokines.

To gain a better understanding of TRAF1, we can also create a TRAF1 mutation that retains the interaction with cIAP2 and fails to bind to LUBAC and assess how this mutation affects the progression of inflammation in vivo and in vitro.

Appendix

Reaction conditions for Reverse Transcription

1ul of Oligo dT (Qiagen) and 1ul of 10mM dNTP (New England Biolabs) were added into diluted RNA, and step 1 of reverse transcription was performed as below:

Step	Temperature	Time
1	65˚C	5 minutes

Table 2. Thermal cycler conditions for reverse transcription step 1

Mixed 2ul of 10x buffer, 0.2 RNAse inhibitor, and 1ul of mmLV and added them into step1 PCR product. Performed step 2 PCR as below:

Step	Temperature	Time
1	37˚C	50 minutes
2	72˚C	15 minutes
3	4˚C	Infinity Hold

Table 3. Thermal cycler conditions for reverse transcription step 2

cDNA was stored at -20˚C once completed.

Reaction conditions for Real-Time PCR

The qPCR was performed as below:

Step	Temperature	Time

Initial Denaturation	95°C	30 seconds
40 Cycles	95°C	10 seconds
	60°C	30 seconds
Fluorescence Measurement		
Melt Curve increment 0.5 °C/s	95°C	10 seconds
	65°C	5 seconds
Fluorescence Measurement		
Hold	4°C	Infinite Hold

Table 5. Thermal cycler conditions for real-time PCR

Reaction conditions for target site amplification

Target site was amplified by following protocol:

Steps	Temperature	Time	Cycles
Enzyme Activation	95°C	10 minutes	1
Denaturation	95°C	30 seconds	40
Annealing	55°C	30 seconds	
Elongation	72°C	30 seconds	
Final Extension	72°C	7 minutes	1
Hold	4°C		

Table 13. Thermal cyclers conditions for TRAF1V203A targeted site amplification

Authors' Contributions

FA identified the interaction site between TRAF1 and c-IAP2 and created the TRAF1V203A mutation. SZ introduced the TRAF1V203A mutation into THP-1 human monocytes by CRISPR/Cas9. Analysis and acquisition of all data in this thesis was done by myself.

References

[1] D. D. Nancy Garrick, 'Rheumatoid Arthritis', National Institute of Arthritis and Musculoskeletal and Skin Diseases, Apr. 20, 2017. https://www.niams.nih.gov/health-topics/rheumatoid-arthritis (accessed Jan. 04, 2023).

[2] D. C. Guttridge, C. Albanese, J. Y. Reuther, R. G. Pestell, and A. S. Baldwin, 'NF-κB Controls Cell Growth and Differentiation through Transcriptional Regulation of Cyclin D1', Mol Cell Biol, vol. 19, no. 8, pp. 5785–5799, Aug. 1999, doi: 10.1128/MCB.19.8.5785.

[3] T. Lawrence, 'The Nuclear Factor NF- B Pathway in Inflammation', Cold Spring Harbor Perspectives in Biology, vol. 1, no. 6, pp. a001651–a001651, Dec. 2009, doi: 10.1101/cshperspect.a001651.

[4] J.-L. Luo, 'IKK/NF- B signaling: balancing life and death - a new approach to cancer therapy', Journal of Clinical Investigation, vol. 115, no. 10, pp. 2625–2632, Oct. 2005, doi: 10.1172/JCI26322.

[5] P. H. Salim and R. M. Xavier, 'Influence of genetic polymorphisms (IL-10/CXCL8/CXCR2/NFκB) on the susceptibility of autoimmune rheumatic diseases', Revista Brasileira de Reumatologia (English Edition), vol. 54, no. 4, pp. 301–310, Jul. 2014, doi: 10.1016/j.rbre.2013.10.005.

[6] M. Karin and M. Delhase, 'The IκB kinase (IKK) and NF-κB: key elements of proinflammatory signalling', Seminars in Immunology, vol. 12, no. 1, pp. 85–98, Feb. 2000, doi: 10.1006/smim.2000.0210.

[7] S. Vallabhapurapu and M. Karin, 'Regulation and Function of NF-κB Transcription Factors in the Immune System', Annu. Rev. Immunol., vol. 27, no. 1, pp. 693–733, Apr. 2009, doi: 10.1146/annurev.immunol.021908.132641.

[8] H. Zhang and S.-C. Sun, 'NF-κB in inflammation and renal diseases', Cell Biosci, vol. 5, no. 1, p. 63, Dec. 2015, doi: 10.1186/s13578-015-0056-4.

[9] F. Guo et al., 'TRAF1 is involved in the classical NF-κB activation and CD30-induced alternative activity in Hodgkin's lymphoma cells', Molecular Immunology, vol. 46, no. 13, pp. 2441–2448, Aug. 2009, doi: 10.1016/j.molimm.2009.05.178.

[10] R. M. Plenge et al., 'TRAF1–C5 as a Risk Locus for Rheumatoid Arthritis — A Genomewide Study', N Engl J Med, vol. 357, no. 12, pp. 1199–1209, Sep. 2007, doi: 10.1056/NEJMoa073491.

[11] A. J. McPherson, L. M. Snell, T. W. Mak, and T. H. Watts, 'Opposing Roles for TRAF1 in the Alternative versus Classical NF-κB Pathway in T Cells', Journal of Biological Chemistry, vol. 287, no. 27, pp. 23010–23019, Jun. 2012, doi: 10.1074/jbc.M112.350538.

[12] H. Guo, J. B. Callaway, and J. P.-Y. Ting, 'Inflammasomes: mechanism of action, role in disease, and therapeutics', Nat Med, vol. 21, no. 7, pp. 677–687, Jul. 2015, doi: 10.1038/nm.3893.

[13] D. K. Stringer and R. C. Piper, 'Terminating protein ubiquitination: Hasta la vista, ubiquitin', Cell Cycle, vol. 10, no. 18, pp. 3067–3071, Sep. 2011, doi: 10.4161/cc.10.18.17191.

[14] D. S. Vinay and B. S. Kwon, '4-1BB signaling beyond T cells', Cell Mol Immunol, vol. 8, no. 4, pp. 281–284, Jul. 2011, doi: 10.1038/cmi.2010.82.

[15] G. S. Firestein, 'Evolving concepts of rheumatoid arthritis', Nature, vol. 423, no. 6937, pp. 356–361, May 2003, doi: 10.1038/nature01661.

[16] M. A. M. van Delft and T. W. J. Huizinga, 'An overview of autoantibodies in rheumatoid arthritis', Journal of Autoimmunity, vol. 110, p. 102392, Jun. 2020, doi: 10.1016/j.jaut.2019.102392.

[17] F. A. S. Kurreeman et al., 'A Candidate Gene Approach Identifies the TRAF1/C5 Region as a Risk Factor for Rheumatoid Arthritis', PLoS Med, vol. 4, no. 9, p. e278, Sep. 2007, doi: 10.1371/journal.pmed.0040278.

[18] C.-Y. Wang, M. W. Mayo, R. G. Korneluk, D. V. Goeddel, and A. S. Baldwin, 'NF-κB Antiapoptosis: Induction of TRAF1 and TRAF2 and c-IAP1 and c-IAP2 to Suppress Caspase-8 Activation', Science, vol. 281, no. 5383, pp. 1680–1683, Sep. 1998, doi: 10.1126/science.281.5383.1680.

[19] M. Biancalana, E. Natan, M. J. Lenardo, and A. R. Fersht, 'NF-κB Rel subunit exchange on a physiological timescale', Protein Science, vol. 30, no. 9, pp. 1818–1832, Sep. 2021, doi: 10.1002/pro.4134.

[20] T. Liu, L. Zhang, D. Joo, and S.-C. Sun, 'NF-κB signaling in inflammation', Sig Transduct Target Ther, vol. 2, no. 1, p. 17023, Jul. 2017, doi: 10.1038/sigtrans.2017.23.

[21] J. Inoue et al., 'Tumor Necrosis Factor Receptor-Associated Factor (TRAF) Family: Adapter Proteins That Mediate Cytokine Signaling', Experimental Cell Research, vol. 254, no. 1, pp. 14–24, Jan. 2000, doi: 10.1006/excr.1999.4733.

[22] T. Zotti, I. Scudiero, P. Vito, and R. Stilo, 'The Emerging Role of TRAF7 in Tumor Development: TRAF7 IN TUMOR DEVELOPMENT', J. Cell. Physiol., vol. 232, no. 6, pp. 1233–1238, Jun. 2017, doi: 10.1002/jcp.25676.

[23] A. Wicovsky, F. Henkler, S. Salzmann, P. Scheurich, C. Kneitz, and H. Wajant, 'Tumor necrosis factor receptor-associated factor-1 enhances proinflammatory TNF receptor-2 signaling and modifies TNFR1–TNFR2 cooperation', Oncogene, vol. 28, no. 15, pp. 1769–1781, Apr. 2009, doi: 10.1038/onc.2009.29.

[24] E. N. Tsitsikov et al., 'TRAF1 Is a Negative Regulator of TNF Signaling', Immunity, vol. 15, no. 4, pp. 647–657, Oct. 2001, doi: 10.1016/S1074-7613(01)00207-2.

[25] D. E. Speiser et al., 'A Regulatory Role for TRAF1 in Antigen-induced Apoptosis of T Cells', Journal of Experimental Medicine, vol. 185, no. 10, pp. 1777–1783, May 1997, doi: 10.1084/jem.185.10.1777.

[26] I. Carpentier and R. Beyaert, 'TRAF1 is a TNF inducible regulator of NF-κB activation', FEBS Letters, vol. 460, no. 2, pp. 246–250, Oct. 1999, doi: 10.1016/S0014-5793(99)01356-3.

[27] I. K. Jang, Z. H. Lee, Y. J. Kim, S. H. Kim, and B. S. Kwon, 'Human 4-1BB (CD137) Signals Are Mediated by TRAF2 and Activate Nuclear Factor-κB', Biochemical and Biophysical Research Communications, vol. 242, no. 3, pp. 613–620, Jan. 1998, doi: 10.1006/bbrc.1997.8016.

[28] R. H. Arch and C. B. Thompson, '4-1BB and Ox40 Are Members of a Tumor Necrosis Factor (TNF)-Nerve Growth Factor Receptor Subfamily That Bind TNF Receptor-Associated Factors and Activate Nuclear Factor κB', Mol Cell Biol, vol. 18, no. 1, pp. 558–565, Jan. 1998, doi: 10.1128/MCB.18.1.558.

[29] F. Cossu, M. Milani, E. Mastrangelo, and D. Lecis, 'Targeting the BIR Domains of Inhibitor of Apoptosis (IAP) Proteins in Cancer Treatment', Computational and Structural Biotechnology Journal, vol. 17, pp. 142–150, 2019, doi: 10.1016/j.csbj.2019.01.009.

[30] K. Schroder and J. Tschopp, 'The Inflammasomes', Cell, vol. 140, no. 6, pp. 821–832, Mar. 2010, doi: 10.1016/j.cell.2010.01.040.

[31] S. Vollmer et al., 'The mechanism of activation of IRAK1 and IRAK4 by interleukin-1 and Toll-like receptor agonists', Biochemical Journal, vol. 474, no. 12, pp. 2027–2038, Jun. 2017, doi: 10.1042/BCJ20170097.

[32] T. Kawai and S. Akira, 'Signaling to NF-κB by Toll-like receptors', Trends in Molecular Medicine, vol. 13, no. 11, pp. 460–469, Nov. 2007, doi: 10.1016/j.molmed.2007.09.002.

[33] A. A. Abdul-Sater, M. I. Edilova, D. L. Clouthier, A. Mbanwi, E. Kremmer, and T. H. Watts, 'The signaling adaptor TRAF1 negatively regulates Toll-like receptor signaling and this underlies its role in rheumatic disease', Nat Immunol, vol. 18, no. 1, pp. 26–35, Jan. 2017, doi: 10.1038/ni.3618.

[34] 'Autoimmune diseases | Office on Women's Health'. https://www.womenshealth.gov/a-z-topics/autoimmune-diseases (accessed Jan. 04, 2023).

[35] R. H. Arch, R. W. Gedrich, and C. B. Thompson, 'Tumor necrosis factor receptor-associated factors (TRAFs)—a family of adapter proteins that regulates life and death', Genes Dev., vol. 12, no. 18, pp. 2821–2830, Sep. 1998, doi: 10.1101/gad.12.18.2821.

[36] T. E. Graber and M. Holcik, 'Distinct roles for the cellular inhibitors of apoptosis proteins 1 and 2', Cell Death Dis, vol. 2, no. 3, pp. e135–e135, Mar. 2011, doi: 10.1038/cddis.2011.20.

[37] G. Goldstein, M. Scheid, U. Hammerling, D. H. Schlesinger, H. D. Niall, and E. A. Boyse, 'Isolation of a polypeptide that has lymphocyte-differentiating properties and is probably represented universally in living cells.', Proc. Natl. Acad. Sci. U.S.A., vol. 72, no. 1, pp. 11–15, Jan. 1975, doi: 10.1073/pnas.72.1.11.

[38] M. H. Glickman and A. Ciechanover, 'The Ubiquitin-Proteasome Proteolytic Pathway: Destruction for the Sake of Construction', Physiological Reviews, vol. 82, no. 2, pp. 373–428, Apr. 2002, doi: 10.1152/physrev.00027.2001.

[39] M. Miranda and A. Sorkin, 'Regulation of Receptors and Transporters by Ubiquitination: New Insights into Surprisingly Similar Mechanisms', Molecular Interventions, vol. 7, no. 3, pp. 157–167, Jun. 2007, doi: 10.1124/mi.7.3.7.

[40] R. M. Locksley, N. Killeen, and M. J. Lenardo, 'The TNF and TNF Receptor Superfamilies', Cell, vol. 104, no. 4, pp. 487–501, Feb. 2001, doi: 10.1016/S0092-8674(01)00237-9.

[41] L. Cabal-Hierro and P. S. Lazo, 'Signal transduction by tumor necrosis factor receptors', Cellular Signalling, vol. 24, no. 6, pp. 1297–1305, Jun. 2012, doi: 10.1016/j.cellsig.2012.02.006.

[42] C. Zheng, V. Kabaleeswaran, Y. Wang, G. Cheng, and H. Wu, 'Crystal Structures of the TRAF2: cIAP2 and the TRAF1: TRAF2: cIAP2 Complexes: Affinity, Specificity, and Regulation', Molecular Cell, vol. 38, no. 1, pp. 101–113, Apr. 2010, doi: 10.1016/j.molcel.2010.03.009.

[43] K. N. Swatek and D. Komander, 'Ubiquitin modifications', Cell Res, vol. 26, no. 4, pp. 399–422, Apr. 2016, doi: 10.1038/cr.2016.39.

[44] M. J. M. Bertrand et al., 'cIAP1 and cIAP2 Facilitate Cancer Cell Survival by Functioning as E3 Ligases that Promote RIP1 Ubiquitination', Molecular Cell, vol. 30, no. 6, pp. 689–700, Jun. 2008, doi: 10.1016/j.molcel.2008.05.014.

[45] L. A. Gravestein and J. Borst, 'Tumor necrosis factor receptor family members in the immune system', Seminars in Immunology, vol. 10, no. 6, pp. 423–434, Dec. 1998, doi: 10.1006/smim.1998.0144.

[46] H. Kumar, T. Kawai, and S. Akira, 'Pathogen Recognition by the Innate Immune System', International Reviews of Immunology, vol. 30, no. 1, pp. 16–34, Jan. 2011, doi: 10.3109/08830185.2010.529976.

[47] P. A. Baeuerle and T. Henkel, 'Function and activation of NF-kappa B in the immune system', Annu Rev Immunol, vol. 12, pp. 141–179, 1994, doi: 10.1146/annurev.iy.12.040194.001041.

[48] S.-C. Sun, 'Non-canonical NF-κB signaling pathway', Cell Res, vol. 21, no. 1, pp. 71–85, Jan. 2011, doi: 10.1038/cr.2010.177.

[49] A. R. Noort, P. P. Tak, and S. W. Tas, 'Non-canonical NF-κB signaling in rheumatoid arthritis: Dr Jekyll and Mr Hyde?', Arthritis Res Ther, vol. 17, no. 1, p. 15, 2015, doi: 10.1186/s13075-015-0527-3.

[50] P. Kaiser and L. Huang, '[No title found]', Genome Biol, vol. 6, no. 10, p. 233, 2005, doi: 10.1186/gb-2005-6-10-233.

[51] M. D. Stewart, T. Ritterhoff, R. E. Klevit, and P. S. Brzovic, 'E2 enzymes: more than just middle men', Cell Res, vol. 26, no. 4, pp. 423–440, Apr. 2016, doi: 10.1038/cr.2016.35.

[52] C. M. Pickart, 'Mechanisms Underlying Ubiquitination', Annu. Rev. Biochem., vol. 70, no. 1, pp. 503–533, Jun. 2001, doi: 10.1146/annurev.biochem.70.1.503.

[53] F. E. Reyes-Turcu, K. H. Ventii, and K. D. Wilkinson, 'Regulation and Cellular Roles of Ubiquitin-Specific Deubiquitinating Enzymes', Annu. Rev. Biochem., vol. 78, no. 1, pp. 363–397, Jun. 2009, doi: 10.1146/annurev.biochem.78.082307.091526.

[54] D. J. Mahoney et al., 'Both cIAP1 and cIAP2 regulate TNFα-mediated NF-κB activation', Proc. Natl. Acad. Sci. U.S.A., vol. 105, no. 33, pp. 11778–11783, Aug. 2008, doi: 10.1073/pnas.0711122105.

[55] S. Vallabhapurapu et al., 'Nonredundant and complementary functions of TRAF2 and TRAF3 in a ubiquitination cascade that activates NIK-dependent alternative NF-κB signaling', Nat Immunol, vol. 9, no. 12, pp. 1364–1370, Dec. 2008, doi: 10.1038/ni.1678.

[56] R. J. Ludwig et al., 'Mechanisms of Autoantibody-Induced Pathology', Front. Immunol., vol. 8, p. 603, May 2017, doi: 10.3389/fimmu.2017.00603.

[57] M. Mellado, 'T cell migration in rheumatoid arthritis', Front. Immunol., vol. 6, 2015, doi: 10.3389/fimmu.2015.00384.

[58] T. Cheng, X. Sun, J. Wu, M. Wang, R. A. Eisenberg, and Z. Chen, 'Increased serum levels of tumor necrosis factor receptor-associated factor 1 (TRAF1) correlate with

disease activity and autoantibodies in rheumatoid arthritis', Clinica Chimica Acta, vol. 462, pp. 103–106, Nov. 2016, doi: 10.1016/j.cca.2016.08.021.

[59] K. Labbé, C. R. McIntire, K. Doiron, P. M. Leblanc, and M. Saleh, 'Cellular Inhibitors of Apoptosis Proteins cIAP1 and cIAP2 Are Required for Efficient Caspase-1 Activation by the Inflammasome', Immunity, vol. 35, no. 6, pp. 897–907, Dec. 2011, doi: 10.1016/j.immuni.2011.10.016.

[60] C. M. Kim et al., 'Crystal structure of TRAF1 TRAF domain and its implications in the TRAF1-mediated intracellular signaling pathway', Sci Rep, vol. 6, no. 1, p. 25526, Jul. 2016, doi: 10.1038/srep25526.

[61] D. Conte et al., 'Inhibitor of Apoptosis Protein cIAP2 Is Essential for Lipopolysaccharide-Induced Macrophage Survival', Mol Cell Biol, vol. 26, no. 2, pp. 699–708, Jan. 2006, doi: 10.1128/MCB.26.2.699-708.2006.

[62] P.-H. Tseng, A. Matsuzawa, W. Zhang, T. Mino, D. A. A. Vignali, and M. Karin, 'Different modes of ubiquitination of the adaptor TRAF3 selectively activate the expression of type I interferons and proinflammatory cytokines', Nat Immunol, vol. 11, no. 1, pp. 70–75, Jan. 2010, doi: 10.1038/ni.1819.

[63] D. Li and M. Wu, 'Pattern recognition receptors in health and diseases', Sig Transduct Target Ther, vol. 6, no. 1, p. 291, Aug. 2021, doi: 10.1038/s41392-021-00687-0.

[64] D. Zheng, T. Liwinski, and E. Elinav, 'Inflammasome activation and regulation: toward a better understanding of complex mechanisms', Cell Discov, vol. 6, no. 1, p. 36, Jun. 2020, doi: 10.1038/s41421-020-0167-x.

[65] N. Kelley, D. Jeltema, Y. Duan, and Y. He, 'The NLRP3 Inflammasome: An Overview of Mechanisms of Activation and Regulation', IJMS, vol. 20, no. 13, p. 3328, Jul. 2019, doi: 10.3390/ijms20133328.